ASSESSMENT OF A NOVEL MATRIX AS A DELIVERY DEVICE FOR ANTIMICROBIALS AND BONE
MORPHOGENETIC PROTEIN-2

by

MARJOLAINE ROUSSEAU

D.M.V., Université de Montréal, 2006
I.P.S.A.V., Université de Montréal, 2007

A THESIS

submitted in partial fulfillment of the requirements for the degree

MASTER OF SCIENCE

Department of Clinical Sciences
College of Veterinary Medicine

KANSAS STATE UNIVERSITY
Manhattan, Kansas

2011

Approved by:

Major Professor
David E. Anderson

Copyright

MARJOLAINE ROUSSEAU

2011

Abstract

Drug delivery systems for time release of recombinant human bone morphogenetic protein-2 (rhBMP-2) and antibiotics in orthopedic surgeries continue to be developed. Recently, a biodegradable novel polymeric matrix has been developed for this purpose. We hypothesized that impregnation of the matrix with rhBMP-2 would enhance bone healing. The objectives of the study were to characterize elution of rhBMP-2 and two antimicrobials (tigecycline, tobramycin) from the matrix, and bone response to the matrix in the presence or absence of rhBMP-2 and antimicrobials.

In vitro elution of tigecycline, tobramycin, and rhBMP-2 from the matrix was investigated. Drug concentration in media were measured on days 1-6, 8, 10, 13, 15, 17, 21, 25, 28, and 30 using high pressure liquid chromatography/mass spectrometry/mass spectrometry (HPLC/MS/MS; antimicrobials) and ELISA (rhBMP-2). *In vivo* testing was done using a unicortical defect created into each tibia of twenty adult goats. Animals were randomly assigned to one of 5 groups: 1) control (untreated defect); 2) matrix; 3) matrix+ antimicrobials (tigecycline+tobramycin); 4) matrix+rhBMP-2; and 5) matrix+antimicrobials+rhBMP-2. Plasma concentration of tigecycline and tobramycin and serum concentration of rhBMP-2 were measured by the above techniques on days 1-7, 9, 11, 13, 15, 17, 22, 26, and 30. Bone response was assessed on days 0, 14, and 30 using radiographic scoring and dual energy X-ray absorptiometry (bone mineral density [BMD]). After euthanasia on day 30, histomorphologic analyses of the bone defects were done. Categorical variables were analyzed using a generalized linear model, and continuous variables using an ANOVA with $P < 0.05$ considered significant.

In vitro elution was characterized by a rapid release on day 1 followed by a slow release until day 30 for both antimicrobials and rhBMP-2. Plasma antimicrobial concentrations showed continued release throughout the study period. Serum rhBMP-2 concentration, radiographic scores and BMD were not significantly different between groups. Periosteal and endosteal reaction surface areas were significantly greater surrounding the defects in group 4

(matrix+rhBMP-2). There was no significant difference between the groups for the percent of bone filling the defect.

The matrix served as an appropriate antimicrobial and rhBMP-2 delivery system and successfully stimulated bone production when rhBMP-2 was present.

Table of Contents

List of Figures

List of Tables

Acknowledgements

Dedication

À mon mari, Kalidou, pour son immense soutien, son amour, et ses encouragements

À mon fils, Zachariah, pour sa grande joie de vivre

Je dédie ce mémoire de maîtrise

List of Abbreviations

ANOVA	analysis of variance
BMD	bone mineral density
BMPs	bone morphogenetic proteins
DEXA	dual energy x-ray absorptiometry
EDTA	ethylenediaminetetraacetic acid
ENDOS:MC	endosteal reaction area:medullary cavity surface ratio
ELISA	enzyme-linked immunosorbent assay
FDA	Food and Drug Administration
HPLC	high-pressure liquid chromatography
HPLC/MS/MS	high pressure liquid chromatography/mass spectrometry/mass spectrometry
LS	least squares (mean)
PLA/PGA	polylactide-polyglycolide
PMMA	polymethylmethacrylate
rhBMP-2	recombinant human bone morphogenetic protein type 2
ROI	region of interest
SEM	standard error of the mean
TGF-β	transforming growth factor-β

Chapter 1 - Introduction

Morbidity associated with open comminuted fractures and secondary osteomyelitis is well recognized. Operative treatments (excision of infected and devascularized tissues, obliteration of dead space, restoration of blood supply and soft-tissue coverage, stabilization and reconstruction of the damaged bone)[1], removal of all foreign bodies and systemic antimicrobial therapy are three crucial components of the treatment of these cases. A long-term course of systemic antibiotherapy has been considered essential, but these prolonged therapies can result in side effects or toxicity. In order to achieve therapeutic drug concentration in the affected bone, high systemic doses are generally required which can further worsen toxic side effects. Despite intensive therapy, advances in surgical techniques, and development of new antimicrobials, relapse rates are still significant and treatment of chronic osteomyelitis remains challenging [2].

A possible adjunct therapy for osteomyelitis is the local delivery of antimicrobial drugs into the site of infection. This approach offers the promises of minimum side effects and maximal bactericidal concentration and effectiveness[3]. In fact, application of local antimicrobials for the treatment of open fractures has been shown to significantly decrease the rate of acute and chronic osteomyelitis in humans[4-6] and in animal models[7,8]. Most carriers used for the local delivery of antimicrobial agents into the bone may be classified into two categories: 1) non-biodegradable and 2) biodegradable[9]. The most commonly used non-biodegradable carrier to locally deliver drugs to bone is polymethylmethacrylate (PMMA) bone cement used to construct antimicrobial impregnated beads[2]. For the last 20 to 30 years, antimicrobial impregnated PMMA implants have been employed in the treatment and prevention of osteomyelitis in humans[9-13] and veterinary patients[14-19]. Antimicrobial impregnated in polymethylmethacrylate (PMMA) has offered local drug delivery with some success. However, the effect of the antimicrobial on the bone cement, the inconsistent elution of the antimicrobial, occasional foreign body reactions to the PMMA, possible development of a biofilm surrounding the cement, and the subsequent need to remove the PMMA beads at the

completion of antimicrobial release drives the need for superior antimicrobial delivery devices[2]. Implantable drug pumps have also been investigated[20, 21] for the treatment of osteomyelitis. More recently, the use of various biodegradable systems for local delivery of antimicrobials has been investigated[12,22]. Biodegradable carriers include collagen sponge[23-25], hydroxyapatite blocks, ceramics and cement[26-32], plaster of Paris beads[33-35], chitosan[36-39], synthetic polymers (e.g. polylactide-polyglycolide (PLA/PGA), polyanhydride, polycaprolactone, dilactate, biomedical polyurethanes)[22,38-41,41-57], fibrin clots[58-63], bone xenograft[64-66], demineralized bone matrix[67], calcium sulfate[3], β-tricalcium phosphate[68-70], hyaluronic acid gel[71], and monolein-water gels[72]. Biodegradable inorganic and organic-inorganic composites have also been explored as antimicrobial delivery devices[73]. Surgical removal of biodegradable carriers becomes unnecessary when their rate of degradation is suitable to the period of release of the antimicrobial and tissue healing. In addition, secondary elution may occur later during the degradation phase of the scaffold, which could offer the benefit of increased antibacterial efficacy compared with that of non-biodegradable carriers. Biodegradable drug delivery vehicles may offer an opportunity to obliterate dead space and guide bone healing[74-78].

Regeneration of bone in traumatic or iatrogenic (orthopedic surgeries and primary tumor resection) critical sized defects, especially if infected, is of major concern to orthopedic surgeons. Large segmental osseous defects are challenging clinical problems. Ideally, secondary osteons progress from one fracture fragment to another when the fragments are in direct contact under compression. In critical sized defects (e.g. > 2-cm), bone replacement becomes necessary to stimulate osteogenesis[2]. Bone can be replaced by biologically similar substances and/or synthetic materials[79]. Cortical and/or cancellous bone autografting (also called autologous or autogenous bone grafts) is the current gold standard treatment of critical-sized bone defects in humans[80] and veterinary patients[80]. Bone autografts first were reported to be used in animals by Merrem in 1810, and in human patients by Philipp von Walther in 1820[81,82]. In current practice, similar bone autografts continue to be the gold standard for bone replacement because they contain the ideal combination of necessary components for bone regeneration: osteoprogenitor cells for osteogenesis, bone matrix for osteoconduction, bone morphogenetic proteins for osteoinduction. Disruption of blood supply to the autograft at the

time of harvest and the high rate of death of the osteoprogenitor cells of both cortical and cancellous bone grafts stimulated the development of vascularized bone grafts. Vascular autografts carried the most favorable biological potential to augment bone union. These pedicle autografts, or free flaps, have been successfully applied for the reconstruction of bone defects in humans[83], but their use is limited. Despite incredible advances in surgical techniques, morbidity associated with graft harvest is well documented in the human literature[84,85]. Donor site morbidity is avoided when using bone allografts and xenografts, but these grafts lack osteoprogenitor cells, have a lower potency for osteoinduction and osteoconduction, and have an increased possibility of non-integration and rejection of the graft[80].

A wide variety of synthetic materials have been designed to replace or augment bone and include metals (e.g. stainless steel 316L, titanium), ceramics (e.g. aluminum oxide, synthetic hydroxyapatite, tricalcium phosphate, etc.), and plastics (e.g. PMMA cement, methacrylate cement, acrylic plastics, polymers such as polylactates and polyglycolates)[86]. Some of these bone substitutes are designed to enhance bone healing or regeneration and are biodegradable (e.g. hydroxyapatite, tricalcium phosphate, polylactates, polyglycolates). These materials can be used alone, or in combination, as carriers for antimicrobials to treat bone infection or provide growth promoting substances to enhance bone healing. Osteostimulatory factors may include bone morphogenetic proteins (BMPs), transforming growth factor-β (TGF- β), platelet-derived growth factors 1 and 2, osteogenic growth peptide, and others[80]. Bone morphogenetic proteins types 2, 4 and 7, and more recently BMP-6 and 9 have been reported to have excellent efficacy inducing bone formation[86]. The BMPs can be extracted from demineralized bone matrix[87-90], but the most recent advance in the production of BMPs is the cloning of recombinant human morphgenetic bone proteins (rhBMPs)[91]. Tissue engineering studies have found that BMPs ideally should be released slowly and gradually, usually from a carrier, at a localized area over several weeks to allow optimized bone formation[92]. Two different BMPs are currently available in the United States for clinical use in humans. The Food and Drug Administration (FDA) has approved in 2002 a recombinant human form of BMP-2 (rhBMP-2) locally delivered by an absorbable purified collagen type I sponge as an autograft replacement for certain interbody spinal fusion procedures[a]. Clinical approval was also granted for the use of this product in open

tibial fractures (2004), and certain oral and maxillofacial bone grafting procedures (sinus augmentations, localised alveolar ridge augmentations; 2007)[86]. Two rhBMP-7 products are approved by the FDA under a Humanitarian Device Exemption and are indicated for use as an alternative to autografts in recalcitrant long bone nonunions[b] and lumbar spinal fusion[c] where use of autologous bone graft is unfeasible or is not expected to promote fusion and alternative treatments have failed. Both product use a purified Type I bovine collagen as the carrier[b,c].

Local delivery of BMPs also was reported to improve healing of open fractures in human patients[93] and infected osseous sites in animal models[94]. These findings most likely are caused by the osteoinductive properties of BMPs, increasing the fracture stability and local vascular supply, and indirectly improving bone healing and local control of osteomyelitis[95,96]. The addition of osteoinductive agents such as rhBMP-2 to antimicrobials to be delivered locally could theoretically be synergistic and allow better and more rapid bone healing.

More recently the use of composite materials that would mimic structures of bone have been investigated because they combine advantages and drawbacks from their components to try to develop the ideal bone drug delivery device for antimicrobials and/or BMPs. Ideally, these composite drug delivery devices should be capable of filling bone defects, providing a conductive scaffold for bone healing, and provide structural support to the injured bone.

Orlumet[d], in collaboration with the Nanotechnology Center[e], has developed a novel polymeric bone matrix that is a biodegradable composite of demineralized bone matrix, polymer, and hydroxyapatite. All of these components are materials already in clinical use and approved by the FDA. This bone grafting scaffold has the potential to be used as a drug delivery system for controlled release of rhBMP-2, growth factors, antimicrobials, and other pharmaceuticals (e.g. antineoplastic agents). This drug-composite matrix possesses osteoconductive and osteoinductive properties with potential future applications in orthopedic and oromaxillary surgeries. This novel bone implant has undergone preliminary testing in oral surgery with success in human subjects[d].

We hypothesized that temporal release of rhBMP-2 impregnated onto the Novel Polymeric Bone Matrix will enhance bone healing with or without temporal release of antimicrobials (tigecycline and tobramycin) also impregnated onto the matrix.

The objective of this study was to determine if the Novel Polymeric Bone Matrix acts as scaffold and appropriate carrier for antimicrobials and growth factors that would stimulate more rapid bone healing. These objectives were investigated using *in vitro* and *in vivo* models. The specific aims of the *in vitro* study were to determine the temporal release of rhBMP-2 and antimicrobials impregnated onto the matrix and to determine if the elution of these substances is affected by co-impregnation of antimicrobials and rhBMP-2. The specific aims of the *in vivo* study were to determine the response of cortical bone to the matrix alone and to the impregnation of antimicrobials or rhBMP-2 onto the matrix, as well as to determine if any interaction occurs with the co-impregnation of antimicrobials and rhBMP-2 onto the matrix. Further, the *in vivo* study was designed to determine systemic exposure of the goats to rhBMP-2, tigecycline and tobramycin when locally delivered by the matrix.

Chapter 2 - Materials & Methods

IN VITRO EVALUATION OF rhBMP-2 AND ANTIMICROBIALS (TIGECYCLINE AND TOBRAMYCIN) ELUTION FROM THE NOVEL POLYMERIC BONE MATRIX

Preparation of the novel polymeric bone matrix

The novel polymeric bone matrix (Figure B.1) was constituted of demineralized bone matrix, hydroxyapatite, and an absorbable polymer. The proprietary information[d,e] of the exact constituents, their characteristics (molecular weight, porosity percent, source) and proportions were unknown by the author at the time of writing. For the *in vivo* experiment, the matrix was manufactured[d,e] in a cylinder with a diameter of 3.5 mm and a length of 1.5 cm to facilitate its insertion into the unicortical bone defect model (*in vivo* experiment). The same configuration was used for the *in vitro* experiment. Based on the formula to compute the volume of a cylinder (Figure B.2), the matrix had a volume of 0.144 cm^3. This volume was necessary for the calculation of the dosage of rhBMP-2 impregnated onto the matrix.

Impregnation of the novel polymeric bone matrix

Reconstitution of the lyophilized rhBMP-2[a] (4.2 mg/vial) was done with sterile water to a final concentration of 0.75 mg/ml. The total volume of rhBMP-2 impregnated onto the matrix was 0.3 ml, which constituted a total dose of approximately 1.5 mg of rhBMP-2 per cm^3 of matrix[97]. The lyophilized powder of tigecycline[f] (50 mg/vial) was reconstituted using 0.9% sodium chloride solution for injection to a concentration of 50 mg/ml. A volume of 0.1 ml of the reconstituted tigecycline, which corresponds to an approximate dose of 5 mg of tigecycline was impregnated onto the matrix. A volume of 0.13 ml of a 40 mg/ml injectable solution of tobramycin sulfate[g] (contained within a multiple dose vial and stored at room temperature) was instilled on the matrix. This corresponded to an approximate dose of 5 mg of tobramycin sulfate.

Impregnation of all drugs was performed by slow instillation onto the matrix using a sterile tuberculin syringe and needle. All products were distributed uniformly across the entire matrix.

Evaluation of the rhBMP-2, tigecycline and tobramycin elution from the bone matrix

Three novel polymeric bone matrixes were used for the *in vitro* experiment. One of them was impregnated with rhBMP-2 (1.5 mg per cm^3 of matrix); the second was impregnated with tigecycline (5 mg) and tobramycin (5 mg); and the third was impregnated with rhBMP-2, tigecycline and tobramycin at the same doses. These impregnated bone matrixes were completely submerged in 10 ml of 0.9% sodium chloride solution (saline) in individual petri dishes with lid and incubated at 37°C (day 0). Supernatant was aspirated with a syringe and needle daily on days 1 through 6 and again on days 8, 10, 13, 15, 17, 21, 25, 28, and 30. After the supernatant had been obtained for analysis and on each day, the matrix and incubation well were rinsed three times with 10 ml of fresh saline. The matrix was then completely submerged in 10 ml of fresh saline before continuing incubation. A new syringe and needle were used between each steps (aspiration, rinse, and re-submersion). The supernatant was transferred to cryotubes and frozen at -80°C until rhBMP-2, tigecycline, and tobramycin assays were performed.

Determination of tigecycline concentration using LC/MS/MS

Frozen supernatant samples were thawed at room temperature. A structurally related antibiotic, minocycline, was used as the internal standard. The analyte (supernatant sample) and spiked internal standard were isolated from 200 μl of saline solution by protein precipitation using acetonitrile. Extracts were filtered using centrifugal filters[h] and then evaporated to dryness at 50°C under nitrogen. The dried extracts were re-constituted in 200 μl of mobile phase A, vortexed and vialed for injection. Electrospray ionization and MS-MS analysis were carried out using a high-pressure liquid chromatography (HPLC) system[i] coupled with a mass spectrometer[j]. Chromatographic separation of analyte and internal standard was

achieved using a C18 analytical column[k] and a gradient elution from 100% mobile phase A (0.2% acetic acid in water) to 95% mobile phase B (0.2% acetic acid in acetonitrile) and re-equilibration over a 5.0 minute runtime. Identification and quantification were based on the following transitions:

Tigecycline	m/z586→m/z456
Minocycline	m/z458→m/z352

The method was proven to be accurate and precise across a linear dynamic range of 1.0-500 ng/ml. The level of quantification was therefore 1.0 ng/ml.

Determination of tobramycin concentration using LC/MS/MS

A structurally related antibiotic, amikacin, was used as the internal standard. The analyte and internal standard were isolated from 200 µl of saline solution by protein precipitation using trichloroacetic acid. Extracts were filtered using centrifugal filters[h] and vialed for injection. Electrospray ionization and MS-MS analysis were carried out using a HPLC system[i] coupled with a mass spectrometer[j]. Chromatographic separation of analyte and internal standard was achieved using a C18 analytical column[k] and a gradient elution from 100% mobile phase A (2mM ammonium acetate, 0.1% formic acid, 10mM heptafluorobutyric acid in water) to 90% mobile phase B (2mM ammonium acetate, 0.1% formic acid, 10mM heptafluorobutyric acid in acetonitrile) and re-equilibration over a 6.0 minute runtime. Identification and quantification were based on the following transitions:

Tobramycin	m/z468→m/z163
Amikacin	m/z586→m/z163

The method was proven to be accurate and precise across a linear dynamic range of 1.0-500 ng/ml. The level of quantification was therefore 1.0 ng/ml.

Determination of rhBMP-2 concentration by sandwich ELISA

Concentration of rhBMP-2 in the supernatant was measured with a commercial rhBMP-2 enzyme-linked immunosorbent (ELISA) kit[l]. The kits were refrigerated at -4°C and all reagents

and samples (supernatant) were brought to room temperature before use. All samples and standards were assayed in duplicate and according to the manufacturer's instructions. The reagents were prepared as follows. Twenty milliliters of wash buffer concentrate was added to distilled water to yield 500 ml of wash buffer. Twenty milliliters of calibrator diluent concentrate was diluted into distilled water to prepare 200 ml of calibrator diluent and was allowed to mix for at least 15 minutes before use. Color reagents A and B were mixed together in equal volumes within 15 minutes of use and protected from light after dissolution. The BMP-2 standard was diluted with 1 ml of distilled water to produce a stock solution of 20,000 pg/ml. The standard was gently agitated for at least 15 minutes before use to make dilutions. A serial dilution was performed from the stock solution to obtained 4000, 2000, 1000, 500, 250, 125, and 62.5 pg/ml of BMP-2. The 4000 pg/mL standard represented the high standard and the calibrator diluent, the zero standard (0 pg/mL).

The assay diluent (100 µl) was added to each well of a plate, followed by the addition of 50 µl of standard, control, or sample. The standards and samples were recorded on a template sheet. The plate was covered and incubated for 2 hours at room temperature on a horizontal orbital microplate shaker set at 500 rpm ± 50 rpm. Using an automatic washer, all wells were aspirated and washed for a total of four washes. The plate was then inverted and blotted against clean paper towels to remove any remaining solution from the wells. A volume of 200 µl of BMP-2 conjugate was added to each well. The plate was then covered and incubated for another 2 hours at room temperature on the same shaker. Four aspiration/wash cycles of the wells were performed. A volume of 200 µl of substrate solution was added to each well before a 30-minute incubation period while protected from light at room temperature on the benchtop. The Stop Solution (50 µl) was then added to each well. The optical density of each well was determined within 30 minutes, using a microplate spectrophotometer[m]. Optical densities were measured with the wavelength set at 450 and 570 nm. All measured values were entered into a spreadsheet[n]. To correct for optical imperfections in the plate, the readings at 570 nm were subtracted from the readings at 450 nm. The average of the corrected duplicate readings for each standard, control, and sample was computed. The average zero standard optical density was then subtracted from each average. A standard curve was generated for

each set of samples assayed. A scatter plot of the optical density for the standards (y axis) versus the concentration of the standards (x axis) was made using a logarithmic axis (y axis) to make the relationship linear. A linear trend line was inserted in the plot. The equation of the linear function and its correlation coefficient (R^2) were displayed. To determine the BMP-2 concentration of each sample, the concentration value (x axis) was calculated for a given optical density, using the computed equation. If the samples were diluted, the concentration read from the standard curve was multiplied by the dilution factor. According to the manufacturer, the minimum detectable dose of BMP-2 ranged from 4.3 to 29 pg/mL (mean: 11 pg/mL).

Statistical analysis

It was decided to perform this pilot *in vitro* experiment in order to better understand the binding of the drugs to and temporal release from the matrix. Due to financial constraints, it was not possible to have replication of the experimental unit (only 1 matrix specimen used per incubation period and drug assayed). Therefore, a statistical analysis was not performed. Descriptive data and graphical representation (concentration of tigecycline, tobramycin and rhBMP-2 vs. time) of the *in vitro* data is presented.

IN VIVO EVALUATION OF THE NOVEL POLYMERIC BONE MATRIX AND EFFECT OF rhBMP-2 AND/OR ANTIMICROBIALS (TIGECYCLINE AND TOBRAMYCIN) IMPREGNATION ON BONE RESPONSE

Animals

The animal model used in this study was approved by the Institutional Animal Care and Use Committee at the Kansas State University (protocol number 2619). Twenty skeletally mature (3 to 5 years old), clinically normal female crossbred goats were used in this study. The goats were determined to be healthy based on the results of physical and lameness examinations. Goats weighed a mean of 34.3 kg [75.5 lbs] (median, 34 kg [74.8 lbs]; range, 17-50 kg [37.4-110 lbs]). All goats were allowed to have an acclimation period of 7 days and were housed in a group of 20 in a dry lot. During the early study period, all goats were housed in groups of 4 to 6 animals and housed in 12 feet X 12 feet [3.7 m x 3.7 m] stalls bedded with pine wood shavings (day 0 through day 17). On day 18 and through the completion of the study (day 30), goats were housed in the dry lot. Goats were fed free choice brome hay and water throughout the study period except when food and water were withheld for 12 hours prior to surgery. The day of surgery was designated as day 0.

Anesthesia

General anesthesia was induced in all goats using a combination of butorphanol tartrate[o] (0.025 mg/kg IV), xylazine hydrochloride[p] (0.05 mg/kg IV) and ketamine hydrochloride[q] (2 mg/kg IV). Endotracheal intubation was performed and anesthesia maintained by the administration of isoflurane[r] gas vaporized into 100% oxygen and delivered using a semi-closed circuit system. Surgical plane anesthesia was maintained by monitoring each goat for signs of spontaneous movement, response to surgical stimulation, palpebral reflex, heart rate, breathing rate, and mandibular muscle tone.

Surgical procedures

Following induction of general anesthesia, goats were placed in dorsal recumbency and the hind limbs attached to the surgery table in abduction and partial extension to allow access to the proximal and medial aspect of both tibias. A No. 40 surgical clipper blade was used to clip the hair of the medial surface of both hind limbs from the distal aspect of the femur to the mid-diaphysis of the tibia. The clipped areas were aseptically prepared using alternating scrub cycles with iodine surgical scrub and 70% isopropyl alcohol.

A 1.5-cm longitudinal skin incision was performed over the craniomedial aspect of the proximal diaphysis of the tibia using a No. 10 scalpel blade. The incision was extended through the periosteum. A 3.5-mm drill bit was inserted through a 3.5-mm tissue protector and drill guide and was drilled through the cis cortex of the tibia. A battery powered, low-speed (< 150 rpm) drill was used to create the defects. One unicortical defect was created in each tibia. Using a Latin Square Design, the goats were completely blindly and randomly assigned to each of the five treatment groups consisting of 4 goats. The bone defect was created but not treated in the control group (group 1 (C)). In the other 4 treatment groups, the bone defect was created and then treated with matrix in group 2 (M), antimicrobial impregnated matrix in group 3 (MAb), rhBMP-2 impregnated matrix in group 4 (MBMP), or antimicrobial and rhBMP-2 impregnated matrix in group 5 (MAbBMP). After implantation of the matrix (groups 2, 3, 4, and 5), periosteum was apposed with No. 2-0 synthetic absorbable suture material and the skin incision was closed with No. 1 synthetic absorbable suture material in interrupted cruciate patterns. The closure of the periosteum and skin incisions was identically performed for group 1. The procedure was repeated on the contralateral tibia. Both tibias of each goat were bandaged and animals were allowed to recover from anesthesia in a transporting pen with rubber flooring until they were able to stand and walk on their own. They were then returned to their original stall.

Impregnation of antimicrobials and rhBMP-2

All surgeries were performed on a total of four mornings. Tigecycline is stable at room temperature for up to 6 hours following reconstitution, therefore a new vial was reconstituted on each day of surgical implantations. Similarly, reconstituted rhBMP-2 is stable at room temperature for several hours and therefore a new vial was reconstituted each morning of surgical implantations.

Intra-operative instillation of tigecycline, tobramycin and rhBMP-2 solutions onto the bone matrix was performed within 10 minutes of implantation using a sterile tuberculin syringe and needle. All products were distributed uniformly across the entire matrix. For group 5, the rhBMP-2 was instilled before the antimicrobials to ensure adequate impregnation.

Postoperative monitoring

Complete physical examinations were performed every 12 hours for a period of 17 days after surgery on all goats and included the assessment of pain, lameness, and evaluation of the surgical site. Appetite, water intake, temperament, activity level, and interactions between the goats were also monitored. Bandages were removed 24 hours postoperatively. On day 14, the skin sutures were removed. Beginning on day 17 and continuing through day 30, the goats were visually inspected once daily to assess appetite, temperament, and behavior.

All goats were allowed to walk and trot in a circle in their stall for lameness evaluation. Hind limb lameness was subjectively assessed twice daily on a scale of 0 to 4 (0 = normal gait; 1 = mild lameness; 2 = moderate lameness; 3 = severe lameness; 4 = catastrophic lameness)[93] for the first 17 days after surgery. Assessment was performed by the author who was blinded to treatment allocation. Based on initial statistical modeling analysis, the lameness scores were subsequently categorized as "0" for normal gait (previous lameness score of 0), and "1" for presence of lameness (previous lameness scores ≥ 1). This was done in order to transform the response variable (lameness) into a binomial distribution. The lameness data was modeled into a generalized linear model and analyzed using the GLIMMIX procedure in statistical analysis software[s].

Radiographic evaluation of bone healing

Radiographic images of the tibias were obtained every 2 weeks beginning the day after surgery (day 1, 14, 30). These images were obtained with the goats under recumbent sedation (xylazine hydrochloride[p] 0.05 mg/kg IV). If needed, sedative effects of the xylazine were reversed by subcutaneous injection of tolazoline hydrochloride[t] (1.5-2.0 mg/kg) at the end of the procedures. Two orthogonal radiographic views (lateral and craniocaudal) of each tibia were obtained using a digital radiography unit[u] and viewed via a computer software program[v]. Bone response surrounding the defects was assessed in two regions: periosteum, and endosteum. For statistical analysis, a subjective scoring system (0 = no reaction; 1 = presence of reaction) was used to assess bone response. A second scale was used to assess presence of excessive bony reaction (2 = absence of excessive reaction; 3 = presence of excessive reaction) in the two regions. On day 1, all scores were assigned a value of 0, and all subsequent images (days 14 and 30) were compared to the day 1 radiographs. Artifacts associated with the implanted matrix were taken into account when evaluating subsequent radiographs (days 14 and 30). All images were evaluated at the end of the study by a reviewer that had been blinded to the treatment groups. The response variables (periosteal and endosteal reactions) were modeled into a generalized linear model with a binomial distribution (GLIMMIX procedure[s]). Significance was set at a *P* value of < 0.05.

Evaluation of bone mineral density

Dual energy x-ray absorptiometry (DEXA) was used to quantitatively measure bone mineral density (BMD) at the site of implantation of the left tibia only. The procedure was performed on days 1, 14, and 30 under recumbent sedation protocol as previously described. Scans were performed at 140 and 70 kVP and a mean of 2.0 mA. Scans were performed in planes perpendicular to the long axis of the bone defect using a single beam with line spacing and point resolution set at 0.10 cm. A region of interest (ROI) 30 mm x 30 mm in area was defined centered on the bone defect. The ROI was then processed to create a bone map which

measured the area (cm^2) and bone mineral content (grams), and calculated the BMD (grams/cm^2). Due to the mineral component of the bone matrix, the initial BMD was measured postoperatively on day 1. A proportional change in BMD (Figure B.3) between days 1 and 14, and days 1 and 30 were then computed by subtracting the initial BMD (day 1) from the BMD on a given day (14 or 30) and dividing this change in BMD by the initial BMD (day 1).

Proportional changes in BMD on days 14 and 30 were compared between treatment groups by performing an analysis of variance (ANOVA) of repeated measures[w]. The variable "goat" was modeled as a random effect (repeated measures) and the variables "treatment groups" and "time" were modeled as fixed effects. Significance was set at a *P* value of < 0.05.

Collection and processing of blood samples

A venous blood sample (8-10 ml) was collected from the jugular vein before the surgery (day 0) and at days 1, 2, 3, 4, 5, 6, 7, 9, 11, 13, 15, 17, 22, 26, and 30 after the implantation. Blood samples were transferred immediately from the syringe into a 10-ml serum tube[x] and a 2-ml ethylenediaminetetraacetic acid (EDTA) coated tube[y] and stored on ice for up to 4 hours. Clotted blood samples were centrifuged[z] at room temperature for 10 minutes at 5000 rpm (1398 x g) to separate serum (serum tube) and plasma (EDTA tube) from the remaining blood components. Serum and plasma were collected, placed in cryotubes, and frozen at -80°C until rhBMP-2 assays (serum) or tigecycline and tobramycin assays (plasma) were performed.

Determination of plasma concentrations of tigecycline and tobramycin using LC/MS/MS

Frozen plasma samples were thawed at room temperature. The analyte and internal standard were isolated from goat plasma. The same LC/MS/MS methods were used to determine plasma concentration of tigecycline and tobramycin as the ones used to measure supernatant concentrations. Only plasma samples from goats in groups 3 (MAb) and 5 (MAbBMP) were analyzed.

Tigecycline and tobramycin plasma concentrations were compared between treatment groups using an ANOVA of repeated measures[w] to determine presence or absence of time effect, treatment effect, and time and treatment interaction. The variable "goat" was modeled as a random effect (repeated measures) and the variables "treatment" and "time" were modeled as fixed effects. Significance was set at a P value of < 0.05. When a treatment effect or an interaction between time and treatment was detected, individual pair-wise comparisons of least squares means was performed using Student's t-test[w].

Determination of serum concentrations of rhBMP-2 by sandwich ELISA

Concentration of rhBMP-2 in the serum samples was measured with a commercial rhBMP-2 ELISA kit[l], as described for the *in vitro* study. Serum samples from goats in all groups were analyzed. Data was also analyzed using an ANOVA of repeated measures followed by Student's t-test to compare least squares means[w].

Bone defect harvest and preparation of histological slides

On day 30, all goats were euthanatized by intravenous injection of pentobarbital sodium[aa]. Then, all tibias were harvested and 1 tibia per goat was randomly chosen for histological slide preparation and further histomorphologic analysis. After removal of the musculature surrounding the tibia, the bone defect was localized and sections of bone were prepared by cutting the tibia transversally about 1 cm proximal and distal to the bone defect. Sections of bone were preserved and shipped to an external laboratory[bb] in a 10% buffered formalin solution.

Histological slides were prepared from non-decalcified bone sections containing the defect with implant *in situ*. Bone specimens were dehydrated in 70-100% ethanol solutions in multiple cycles for various amount of time (6 to 34 hours), then infiltrated and embedded with histological resin[cc]. Specimens were sectioned with a commercial cutting and grinding system[dd] and stained with toluidine blue O. Sections were obtained in a transverse plane, perpendicular to the long axis of the bone, and traveling through the bone defect and implant *in situ*.

Histomorphologic analysis

Three methods were used to evaluate the quantity of the bony response to the bone trauma and matrix. First, a subjective gross evaluation of the periosteal and endosteal reactions was performed with a reviewer blinded to the treatment groups. A subjective scoring system was used (1 = none or minimal reaction, 2 = moderate or marked reaction). The response variables (periosteal and endosteal reactions) of the gross evaluation of the histological slides was modeled into a generalized linear model with a binomial distribution using the GENMOD procedure[s]. The probability that the endosteal and periosteal reactions were absent or minimal for each treatment groups was also computed.

Secondly, a qualitative gross evaluation of the periosteal and endosteal reactions was performed. Using a digital caliper with a precision of 10 micrometers, the width and length of the periosteal reaction were measured from each histological slide. The surface area (mm^2) of the bone reaction was computed by multiplying its width by its length. The procedure was repeated for the endosteal reaction surface. Furthermore, the width and length of the medullary cavity was measured and its surface area was similarly computed. An estimation of the medullary cavity surface covered by endosteal reaction was computed by dividing the estimated surface of endosteal reaction by the estimated surface of medullary cavity (ENDOS:MC ratio). Surfaces of periosteal and endosteal reactions as well as ENDOS:MC ratios were compared between treatment groups using a 1-way ANOVA[w]. When a significant difference was found, pair-wise comparisons of least squares means were performed using Student's *t*-test[w].

Computerized images of the cortical defects seen on the histological slides were taken via light microscopy[ee] coupled to a digital camera[ff] at 2X magnification. Using image analysis software[gg], the computerized images were split into red, green, and blue channeled images to allow further analysis. For the red channeled images, an area of interest was defined on the approximate margins of the cortical defect. The system then processed the image to measure the surface of the area of interest (μm^2), and calculated the percent of the area that was filled

with bone and/or matrix. The procedure was repeated for the green and blue channeled images. The protocol used for this software is described in Appendix C. For each set of channeled images (red, green, and blue), the effect of treatment groups was analyzed using a 1-way ANOVA[w]. The level of significance was $P < 0.05$. When significance was reached, pair-wise comparisons were done between all treatment groups using Student's t-test[w].

Chapter 3 - Results

IN VITRO EXPERIMENT

In vitro elution of tigecycline

The greatest tigecycline elution was at the beginning of the experiment for the antimicrobials impregnated matrix (49,800 ng/ml). The day 1 sample for the co-impregnated matrix was lost and was not included in the data set. The elution of tigecycline from the antimicrobial impregnated and the co-impregnated matrix slowly decreased throughout the study period (Figures B.4 and B.5) and the smallest concentration was detected on day 30 (248 ng/ml and 360 ng/ml, respectively; Table A.1).

In vitro elution of tobramycin

The greatest tobramycin concentration was measured at the beginning of the experiment for the antimicrobial impregnated matrix (125,000 ng/ml). There was a missing sample from day 1 and insufficient sample volume in a sample from days 2 and 3. These data points were not included in the analysis. The tobramycin elution from the antimicrobial impregnated matrix and co-impregnated matrix rapidly decreased until day 8 at which time the elution slowly decreased until the end of the experiment to concentration of 23.4 ng/ml and 6.1 ng/ml, respectively, on day 30 (Figures B.6 and B.7; Table A.1).

When comparing the supernatant concentrations of tigecycline and tobramycin, the concentration of tigecycline was greater than that of tobramycin at all time points (Table A.1).

In vitro elution of rhBMP-2

The greatest rhBMP-2 elution was at the beginning of the experiment for the rhBMP-2 impregnated matrix (922,800 pg/ml; day 1). It was not possible to measure the rhBMP-2 elution from the co-impregnated (rhBMP-2 and antimicrobials) matrix due to the missing sample (day 1). The rhBMP-2 elution from the co-impregnated matrix remained relatively constant from day

4 and throughout the experiment (Figure B.8). This is in contrast with the supernatant concentration of rhBMP-2 that suddenly increased on days 13 (298,880 pg/ml) and 15 (450,880 pg/ml). For all time points, the concentration of rhBMP-2 in the supernatant of the rhBMP-2 impregnated matrix was greater than that for the co-impregnated matrix (Table A.1).

IN VIVO EXPERIMENT

Surgical procedures and postoperative monitoring

All surgical procedures and recoveries were uneventful. It was noted that the consistency of the polymeric matrix was variable between samples. Subjectively, insertion of the matrix within the bone defects was uneventful when the matrix kept its integrity. Insertion was found to be more difficult to realize due to breakage of the matrix in other goats.

Physical examination parameters, appetite, water intake, temperament, activity level, and interactions between the goats remained within normal limits throughout the study period in all groups. The statistical modeling used for lameness score analysis did not converge; therefore descriptive statistics are used here. Lameness (score ≥ 1) from at least one hind limb was detected on all goats at least once during the study (Tables A.2 to A.6), with the majority of goats having multiple episodes of unilateral or bilateral lameness within the first 7 days of the study period. Only 4 goats (2 from group 1, one from group 2, and one from group 3) had a lameness affecting only one hind limb detected at less than four time points. Lameness was detected at a total of 233 time points from which 80.7% (188/233) were of score 1, 15.4% (36/233) of score 2, and 3.9% (9/233) of score 3.

Radiographic evaluation

The loss of radiographic images from all goats in groups 2 and 3 was caused by digital data corruption. It was not possible to perform statistical analysis on data from day 14. On day 30, no significant differences were detected among treatments for all radiographic scores evaluated (periosteal reaction, endosteal reaction, excessive periosteal reaction, and excessive endosteal reaction; P = 0.986, 0.760, 0.180, and 0.870, respectively; Table A.7).

Bone mineral density

On day 1, the mean BMD was 0.701 g/cm^2, 0.585 g/cm^2, 0.814 g/cm^2, 0.695 g/cm^2, and 0.931 g/cm^2 for groups 1, 2, 3, 4, and 5, respectively (Table A.8). On day 14, the mean BMD was 0.629 g/cm^2, 0.513 g/cm^2, 0.828 g/cm^2, 0.571 g/cm^2, and 0.803 g/cm^2 for groups 1, 2, 3, 4, and 5, respectively (Table A.8). On day 30, the mean BMD was 0.603 g/cm^2, 0.632 g/cm^2, 0.900 g/cm^2, 0.597 g/cm^2, and 0.810 g/cm^2 for groups 1, 2, 3, 4, and 5, respectively (Table A.8). On days 14 and 30, the percent change in BMD did not differ significantly among the groups (P = 0.864) and days (P = 0.362).

Plasma concentrations of tigecycline and tobramycin

Statistical analysis revealed a significant change in mean plasma concentrations of tigecycline over time (P < 0.0001) for groups 3 (MAb) and 5 (MAbBMP). Treatment effect was not significant (P = 0.396), and a no significant interaction between time and treatment (P = 0.653) was found. The results are represented with a single curve (Figure B.12) due to the absence of treatment and interaction effects. The highest mean plasma concentration of tigecycline (3.8 ± 0.3 ng/ml) was noted on day 1. The mean plasma concentration of tigecycline achieved a relative plateau at approximately 3.0 ng/ml on day 2 until day 17 before slowly decreasing until the end of the study period. A mean of 0.974 ± 0.270 ng/ml of tigecycline, which is below the minimal level of quantification (1.0 ng/ml), was detected at the end of the experiment (day 30; Table A.11).

Statistical analysis revealed a significant change in mean plasma concentration of tobramycin over time (P < 0.0001) and a significant interaction between time and treatment (P = 0.0001). However, no treatment effect was detected (P = 0.074). The results are represented with two curves (Figure B.13) to demonstrate the different effect of time for both treatment groups (interaction). In group 3 (MAb), mean plasma concentrations of tobramycin between day 1 and day 4 were constant with values between 1.9 ± 0.6 and 2.0 ± 0.5 ng/ml. The peak concentration was delayed for group 3 (MAb) as compared to group 5 (MAbBMP). In fact, the

mean plasma concentration of tobramycin was the highest on day 1 (4.9 ± 0.4 ng/ml) and day 6 (5.0 ± 0.4 ng/ml) for groups 5 (MAbBMP) and 3 (MAb), respectively (Table A.11). The mean plasma concentration of tobramycin remained constant between day 7 and day 26 in group 5 (MAbBMP) with mean values between 2.4 ± 0.5 and 2.7 ± 0.5 ng/ml. However, mean plasma concentrations of tobramycin in goats of group 3 (MAb) slowly decreased to a mean of 1.6 ± 0.5 ng/ml at the end of the study period (day 30; Table A.11).

Serum concentration of rhBMP-2

Statistical analysis revealed a significant change in serum concentration of rhBMP-2 over time (P < 0.0001) and a significant interaction between time and treatment (P < 0.0001). However, no treatment effect was detected (Figure B.12; P = 0.402) between the five treatment groups (C, M, MAb, MBMP, MAbBMP). The two highest serum concentrations of rhBMP-2 were detected on day 7 in group 1 (C; 111.2 ± 8.0 pg/ml) and day 22 in group 3 (MAb; 111.0 ± 7.9 pg/ml) and were significantly higher than mean pre-implantation values (day 0) of all groups. Initially, the rhBMP-2 concentration detected in the serum rapidly declined over the course of 3 days (groups C, M, MAb, and MBMP) or 4 days (group MAbBMP) post-implantation to achieved concentrations between 15.3 and 23.4 ± 7.9 pg/ml. A rapid increase in the serum concentration was then measured until days 5 to 7 in all groups (concentrations between 93.9 and 111.2 ± 7.9 pg/ml). This was followed by a sudden decrease and achievement of a relative plateau serum concentration of rhBMP-2 for all groups from day 9 to the end of the study (day 30) with values between 28.1 and 61.5 ± 7.9 pg/ml (Table A.15; Figure B.14).

Histomorphologic analysis

No treatment effect was found for the amount of periosteal reaction determined by subjective gross evaluation of histological slides due to non convergence of the statistical model (Table A.17). Subjective gross evaluation of the endosteal reaction as seen on histological slides was significantly different between treatment groups (P = 0.0032; Table A.18).

Mean surface area of the periosteal reaction was significantly greater in group 4 (70.76 ± 10.97 mm^2; P = 0.03) as compared to groups 1 (28.98 ± 10.97 mm^2), 2 (26.65 ± 10.97 mm^2), and 3 (16.92 ± 10.97 mm^2), but was similar to mean surface of periosteal reaction surrounding unicortical defect of goats from group 5 (41.62 ± 10.97 mm^2; Table A.20; Figure B.15).

Mean surface area of endosteal reaction was significantly greater in group 4 (95.30 ± 5.79 mm^2; P < 0.0001) than the other groups, whereas mean surface area of endosteal reaction was significantly lower in group 1 (0.89 ± 5.79 mm^2; Table A.20; Figure B.15). Surface area of ENDOS:MC ratio was larger in group 4 (0.6454 ± 0.0732 mm^2; P = 0.0002) than groups 1 (0.0072 ± 0.0732 mm^2) and 5 (0.3970 ± 0.0732 mm^2). Group 1 also had a significantly lower ratio than any other groups (Table A.20; Figure B.16).

Statistical analysis of the red and green channeled images revealed no significant treatment effect on the mean percent of filled bone defect (P = 0.2981, and 0.1598, respectively; Table A.26; Figure B.17). There was a significant difference between treatment groups (P = 0.0160) with the blue channeled images of the cortical defect (Figures B.18). The percent filling was greater in group 2 (M) than groups 1 (C) and 4 (MBMP) and similar to groups 3 (MAb) and 5 (MAbBMP).

Microscopic scanning of all histological slides did not reveal any signs of inflammation or infection.

Chapter 4 - Discussion

Bone healing in presence of the matrix

Based on the results of this study, the novel polymeric bone matrix successfully stimulated bone healing and served as an effective drug delivery device. This novel polymeric bone matrix contained components, including demineralized bone matrix and hydroxyapatite, that are expected to enhance bone healing. Demineralized bone matrix has been shown to have osteoinductive characteristics due to numerous growth factors made available during dissolution of the inorganic matrix of bone[98]. Hydroxyapatite has been shown to have osteoconductive and perhaps osteostimulatory characteristics in bone[99]. Various polymers have been investigated for use as bone drug delivery devices for growth factors and antimicrobials, not always with success. Polymers may have a positive effect by delivering drugs of benefit to tissue healing[99]. Polymers may also have an inhibitory effect by interfering with tissue ongrowth and ingrowth into the defect[100]. In our goat model, the novel polymeric bone matrix stimulated significantly more new bone formation, as compared to the control group. This effect was greatly enhanced by the presence of rhBMP-2. Interestingly, the effect of the rhBMP-2 seemed to be moderated somewhat by the presence of tigecycline and tobramycin. This may have been caused by competitive binding of the various drugs or may have been associated with local inhibition of osteoblasts.

Elution kinetics

Based on the results of the preliminary *in vitro* experiment, the novel polymeric bone matrix is a potential drug-delivery system for tigecycline, tobramycin and rhBMP-2. Elution was characterized by a rapid release of both antimicrobials studied during the first 24 hours followed by a slower elution rate during the following 30 days. The initial rapid release was probably due to the presence of the unbound proteins on the surface[100] and within the micropores of the matrix. These molecules entered into solution almost immediately on immersion.

Elution of tigecycline from the novel polymeric bone matrix was similar to that reported from a nanoparticle composite[100]. The release kinetics of tobramycin were similar to that reported in other *in vitro* studies of non-biodegradable and biodegradable carriers (Table A.28).

Although statistical analysis was not possible due to the absence of sample replication, presence of rhBMP-2 co-impregnated with antimicrobials did not appear to change the release kinetics of the antimicrobials in our study. The release kinetics of rhBMP-2 was also similar to those reported in other rhBMP-2 elution studies from biodegradable synthetic polymers[101], composites[102] and implant coatings[103,104] under *in vitro* conditions.

Drug release from a carrier system depends on numerous factors, such as the area of exposure, dissolution pattern, distribution within the matrix, and type of bond it forms on the carrier's surfaces[100, 105, 106]. In our *in vitro* experiment, co-impregnation with antimicrobials appeared to change the elution of rhBMP-2 and this may have been associated with competitive binding in the matrix. However, sustained release of rhBMP-2 was achieved in the presence of antimicrobials. In fact, results from *in vitro* studies indicated that exogenous growth factors, such as rhBMP-2, should be delivered locally during a suitable period to allow complete osteoblastic differentiation of mesenchymal cells[107,108].

Comparison between *in vitro* and *in vivo* release profiles of rhBMP-2 is difficult because the *in vivo* release and retention mechanisms involve aqueous hydrolysis as well as enzymatic and cellular events, whereas *in vitro* elution is largely based on aqueous hydrolysis[108-110]. Bioactivity retention of rhBMP-2 was evaluated during the *in vivo* experiment; however, antimicrobial activity retention of tigecycline and tobramycin were not investigated. A change in carrier material can change the pharmacokinetics and effectiveness of the BMPs[111] and antimicrobials. New bone formation was adequately produced in presence of the rhBMP-2-impregnated matrix which confirmed the conservation of osteoinductive properties of rhBMP-2.

Choice of antimicrobials

The most frequent bacterial pathogens implicated in chronic osteomyelitis in humans are the Gram-positive pathogens *Staphylococcus aureus* and group A β-hemolytic *Streptococcus*, and the Gram-negative pathogens such as *Salmonella* spp., *Mycobacterium tuberculosis* and *Pseudomonas aeruginosa*[111]. Antimicrobials most often selected based on desired spectrum for these organisms include aminoglycosides, β-lactams, and fluoroquinolones. These classes of drugs are widely studied antimicrobials for local delivery to bone [1, 112-114]. Recently, *in vitro* activity of novel antimicrobial classes such as glycylcyclines (e.g. tigecycline), oxazolidinones (e.g. linezolid), and cyclic lipopeptides (e.g. daptomycin) against various clinical strains of resistant staphylococci isolated from bone infections have been tested. All isolates were susceptible to tigecycline except one methicillin-resistant *Staphylococcus epidermidis* isolate[2]. Moreover, *in vitro* elution studies of these new anti-infective drugs in relation to various local delivery devices, studies on their antimicrobial efficacy when locally delivered to the bone, and local toxicity studies are limited[115]. Antimicrobial drugs selected for use in local delivery systems should be active against the most common bacterial pathogens involved in osteomyelitis, have a limited systemic absorption, have no toxic effects on cells involved in healing (e.g. endothelium, osteoblasts, osteoclasts, fibroblasts, etc), be safe to use (no adverse effects), be stable at normal body temperature, and be hydrosoluble for adequate diffusion from the carrier[70,101,116].

Tigecycline is the only marketed member of the new glycylcycline family of antimicrobials[2]. This semisynthetic bacteriostatic drug received approval for complicated skin and skin structure infections, complicated intra-abdominal infections, and community-acquired bacterial pneumonia from the FDA in 2005[f,117]. The molecular structure of tigecycline is characterized by the addition of a t-butylglycylamido group at the C-9 position on the central skeleton of minocycline[117] which confers an extended spectrum of activity (Gram-positive and Gram-negative aerobic bacteria and anaerobic and atypical bacteria, including resistant microorganisms) as compared to other tetracyclines. Tigecycline has limited activity against *Pseudomonas aeruginosa* and *Proteus mirabilis*[117]. It acts by inhibiting protein synthesis in susceptible microorganisms by binding to receptors on the 30S subunit of the bacterial

ribosome preventing the addition of amino acids to the elongating peptide chain[118]. Tigecycline has been reported to be effective in the systemic treatment of methicillin-resistant *Staphylococcus aureus*-induced tibial osteomyelitis in a rabbit model[117]. Tigecycline was chosen in our study because of its large spectrum of activity including multi-resistant bacteria as well as its potential to treat osteomyelitis in complicated fractures in humans.

Tobramycin is an aminoglycoside structurally related to kanamycin with bactericidal and pharmacokinetic properties similar to gentamicin. It has dose (concentration) dependent activity primarily against aerobic, Gram-negative bacteria. It has been estimated to have up to four times the activity of gentamicin against *Pseudomonas* spp.[119], which is a significant addition to the spectrum of activity of tigecycline. Tobramycin acts by bacterial ribosomal binding of the 30S and 50S subunits. Due to the resulting prevention of formation of the 70S complex, mRNA cannot be translated into protein. Relative risk for acute renal tubular necrosis, and cochlear and vestibular toxicities appear slightly decreased with systemic usage of tobramycin as compared to other aminoglycosides such as gentamicin and kanamycin[120].

Over the years, researchers have employed various classes of antimicrobials to locally deliver bactericidal concentrations of drugs to normal or affected bone using *in vivo* models and clinical patients. A combination of tigecycline and tobramycin was chosen in our study for multiple reasons. Tobramycin represents a commonly used aminoglycoside and is widely used for local delivery to bone of human patients in the United States because of its spectrum of activity and its availability as a powder[121]. It has been shown to be efficient at concentrations that are not toxic to bone cells[1,2,122,123]. Tigecycline has shown promise with treatment of infected bone in animal models[3,122]. Furthermore, tigecycline has an enhanced spectrum of activity against resistant pathogens[115] involved in clinical cases of osteomyelitis in humans.

Local bone toxicity of antimicrobials

Concerns have been raised regarding the *in vitro* effect of tigecycline on human osteoblast viability in culture. Concentrations of 10 µg/ml appeared to suppress osteoblast cell proliferation[124-126]. In our study, we were not able to investigate the local concentrations of

tigecycline achieved in the interstitial fluids surrounding bone defect after implantation of the matrix. The effect of different concentrations of tigecycline on local bone metabolism as well as surrounding tissues has not been reported in the literature to the author's knowledge.

Local delivery of aminoglycosides have been reported to achieve local concentrations that are > 600 times what is considered toxic in serum without developing systemic toxicity or side effects[127]. However, the result of an experimental study on the effects of tobramycin on human osteoblast-like cells and rat osteoblasts demonstrated that local levels of 400 µg/ml significantly reduced osteoblast replication, and concentrations of 10,000 µg/ml caused cell death; but concentrations ≤ 200 µg/ml had minimal to no effect on cell replication[128]. Another study found that tobramycin at doses > 2000 µg/ml severely decreased cellular proliferation of osteoblasts and chondrocytes[122]. In our study, the peak concentration of tobramycin eluted from the matrix during the preliminary *in vitro* experiment was 125 µg/ml. This concentration likely overestimates the concentration that would be achieved at the implantation site because of interstitial fluid fluxes, and is expected to have little to no effect on replication of osteoblasts.

Systemic exposure to tigecycline and tobramycin

Systemic exposure to tigecycline was minimal in our goat model. According to the product insert[f], the maximal serum concentration of tigecycline is between 0.63 and 1.45 µg/ml and the minimal trough serum concentration of tigecycline at 12 hours is 0.13 µg/ml after intravenous administration of 100 mg in humans. By comparing these pharmacokinetic parameters to the mean maximal serum concentration (day 1) in our model, we can conclude that the peak serum concentration was approximately 32 times lower than the expected minimum serum concentration after parenteral administration in humans. Hence, tigecycline concentrations did not reach therapeutic range systemically and toxicity was consequently avoided.

Monitoring of serum concentrations of aminoglycosides to reduce toxicity and confirm therapeutic concentrations has been described in human[129] and veterinary[130,131] medicine.

Elevated trough concentrations is one of the risk factors for aminoglycoside toxicity[132]. It is thought that trough concentrations of tobramycin greater than 5 µg/ml contribute to nephrotoxicity[133]. Since the highest serum concentration of tobramycin was 4.9 ± 0.4 ng/ml, systemic exposure to tobramycin was low and toxic concentrations were not reached systemically in this caprine model.

Systemic exposure to rhBMP-2

According to the product insert[i], the rhBMP-2-specific sandwich ELISA kit utilized recognizes recombinant and natural BMP-2 from human, rat, and mouse serum. This assay has not been validated for use with goat serum[hh]. Cross-reactivity of the test for different species rhBMP-2 is expected to be good when a similarity of > 80% in the amino acids composing BMP-2 molecule occur[hh]. It is well established that the amino acid sequences of BMP-2 is highly evolutionarily conserved between species of mammals[134]. In a more recent study this finding was specifically confirmed for the BMP-2 protein sequences of three breeds of goats[135]. Hence, it is very likely that the similarity between the amino acid sequences of the caprine BMP-2 molecule and the human BMP-2 is greater than 80%; therefore, the test used was most likely able to detect endogenous caprine BMP-2 molecules as found by the serum concentrations measured preoperatively from all groups, and in groups not treated by BMP-2- impregnated matrix. According to the manufacturer's instruction[i], a standard curve was constructed using known serial concentrations between 62.5 and 4000 pg/ml. Extrapolation of optical densities outside the standard curve can result in false detection of rhBMP-2. This is not a problem in the presence of high concentrations that can be diluted before performing the assay. In our study, most of the concentrations of BMP-2 measured were below the limit of the standard 62.5 pg/ml. Thus, it is difficult to make conclusions as to the actual concentrations in these goats.

Mean serum concentration of rhBMP-2 was found to be increased after surgery at two time points. Interestingly, these findings were from groups not treated with rhBMP-2- impregnated matrix (groups C and MAb). Possible explanations may reside in a sudden release

of endogenous BMP-2 from the bone trauma site, a cross reaction or interference with another molecule, or a technical error with the assay.

Systemic and local toxic effects and adverse reactions associated with the use of rhBMP-2 have not been observed in human or animal studies. This is most likely due to the short half-life and rapid clearance of BMP-2 resulting in minimal systemic exposure[136].

Compatibility between BMP-2 and antimicrobials

The *in vitro* and *in vivo* compatibility of BMPs and antimicrobials have been previously investigated. Kawaguchi *et al.* found that the local delivery of tobramycin in aqueous solution or impregnated in PMMA beads does not affect the osteoinductive properties of rhBMP-7 in a rat model of ectopic bone formation[137]. Suzuki *et al.* reported that the local application of teicoplanin had no inhibitory effect on the ability of locally delivered rhBMP-2 to heal rat calvarial defects[138]. These two studies looked at ectopic and calvaria bone formation which occurs through intramembranous ossification whereas long bone healing occurs through endochondral ossification. Another study[139] found a dose-dependent inhibition of alkaline phosphatase induction and calcium deposition by human mesenchymal stem cells cultured under osteogenic conditions. This inhibition was reversed with the addition of rhBMP-2 at the concentration of 500 ng/ml. During the *in vivo* experiment of that same study[140], tobramycin did not impair the ability of rhBMP-2 to heal non infected critical-sized femoral defects in a rat model. The results of the study reported here are not in complete accordance with that study. Presence of tigecycline and tobramycin co-impregnated into the novel polymeric bone matrix appeared to have affected the ability of rhBMP-2 to enhance bone healing in this goat unicortical tibia defect as determined by a lower endosteal reaction surface area. However, based on the radiographic scores, BMD, and other histomorphologic parameters measured, presence of antimicrobials did not affect the BMP-2-induced new bone formation *in vivo*.

Study limitations

A limitation in the *in vitro* experiment was the absence of replication of the experimental unit which limited statistical analysis. Furthermore, even though local toxicity of the two antimicrobials used in this experiment has been tested, the local toxicity of the combination of both has not been evaluated. Additionally, the antimicrobial activity of the antimicrobials, individually or in combination, was not evaluated.

Goats have been used as animal models for cartilage, meniscal and ligamentous repair, and for testing implantation of biomaterials in bone[140]. Caprine bone metabolic and remodeling rates[141, 142] are similar to those of humans. Tibial blood supply of goats is also similar to the human tibial blood supply[143, 144]. Recommended dimensions of cylindrical implants in the caprine femur or tibia are 4 mm in diameter and 12 mm in length[145]. The tested implant in the present study had similar dimensions. A unicortical tibial defect model of suitable dimensions to accommodate the bone implant was used to test the novel polymeric bone matrix and was chosen as an initial test. In order to evaluate the full potential of this implant, a critical-sized cortical defect model (> 2 times the diaphyseal diameter) would be necessary.

A relatively small number of goats (4) were allocated per treatment group. This probably resulted in our difficulties to detect significant differences between the treatment groups and discrepancy between the results of the different bone healing evaluation methods (radiographic evaluation, BMD assessment, and histomorphologic analysis).

Another limitation in this *in vivo* experiment was the duration of the study period. At the end of the study period (30 days), the bone defects were not completely healed and the novel polymeric bone matrix was not completely absorbed. This resulted in difficulties to evaluate the quality and quantity of new bone formation.

Conclusions

Based on the results of this study, the novel polymeric bone matrix served as an effective carrier for rhBMP-2. Defects treated with the matrix containing rhBMP-2 formed significantly more bone that that of controls and defects that contained only matrix or matrix

and antimicrobials. Interestingly, the matrix in all forms studied, stimulated greater endosteal new bone formation than controls. The matrix allowed release of antibiotics for at least 30 days after implantation. The elution curve was similar to other drug delivery devices with a rapid elution phase initially, followed by a relative plateau. Antibiotics and rhBMP-2 can be used in concert, but the presence of antibiotics may affect the performance of rhBMP-2. The novel polymeric bone matrix can serve as an excellent drug delivery system for the elution of antibiotics and growth factors.

Footnotes

a. INFUSE Bone Graft, Medtronic Safamor Danek, Inc., Minneapolis, Minnesota, 55432.
b. OP-1 Implant, Stryker Biotech, Hopkinton, Massachusetts, 01748.
c. OP-1 Putty, Stryker Biotech, Hopkinton, Massachusetts, 01748.
d. ORLUMET LLC., Little Rock, Arkansas, 72116.
e. Nanotechnology Center, University of Arkansas at Little Rock, Little Rock, Arkansas, 72204.
f. Tigacyl, Wyeth Pharmaceuticals, Inc., Philadelphia, Pennsylvania, 19101.
g. Tobramycin Injection USP, SICOR Pharmaceuticals, Inc., Irvine, California, 92618.
h. Ultrafree-MC Centrifugal Filter Units with Microporous Membrane, Millipore, Inc., Billerica, Massachusetts, 01821.
i. Shimadzu HPLC system, Shimadzu North America / Shimadzu Scientific Instruments, Inc., Columbia, Maryland, 21046.
j. Sciex API 4000 Triple Quadrupole Mass Spectrometer, AB SCIEX, Inc., Foster City, California, 94404.
k. XBridge Shield RP18 Column, Waters Corporation, Milford, Massachusetts, 01757.
l. Quantikine BMP-2 Immunoassay, R&D Systems, Inc., Minneapolis, Minnesota, 55413.
m. Spectra MAX 190, Molecular Devices, Sunnyvale, California, 94089.
n. Microsoft Office Excel 2007, Microsoft Corporation, Redmond, Washington, 98052.
o. Butorphic Injection, 10 mg/ml, LLOYD Laboratories, Inc., Shenandoah, Iowa, 51601.
p. AnaSed Injection, 20 mg/ml, LLOYD Laboratories, Inc., Shenandoah, Iowa, 51601.
q. KetaVed, 100 mg/ml, Vedco, St. Joseph, Missouri 64507.
r. ISOFLURANE USP, Abbott Laboratories, Abbott Park, Illinois, 60064.
s. SAS 9.1.3, SAS Institute, Inc., Cary, North Carolina, 27513.
t. Tolazine Injection, 100 mg/ml, LLOYD Laboratories Inc., Shenandoah, Iowa, 51601.
u. Rapid Study EDR3 Mark III, Eklin Medical Systems, Inc., Santa Clara, California, 95054.
v. AGFA Web1000, Agfa Corporation, Ridgefield Park, New Jersey, 07660.
w. JMP 8.0.1, SAS Institute, Inc., Cary, North Carolina, 27513.
x. BD Vacutainer Serum, BD Diagnostics, Franklin Lakes, New Jersey, 07417.
y. BD Vacutainer K_2EDTA 3.6mg, BD Diagnostics, Franklin Lakes, New Jersey, 07417.
z. International Clinical Centrifuge model CL, International Equipment Co., Needham Heights, Massachusetts, 02494.
aa. Fatal-Plus, 390 mg/ml, Vortech Pharmaceuticals, Ltd., Dearborn, Michigan, 48126.
bb. Purdue Histology and Phenotyping Laboratory, Hard Tissue Section, Medical Discovery and Research Unit, School of Veterinary School, Purdue University, West Lafayette, Indiana, 47907.
cc. Technovit 7200 VLC, Heraeus Kulzer GmbH, 61273 Wehrheim, Germany.
dd. Exakt cutting-grinding system, EXAKT Technologies, Inc., Oklahoma City, Oklahoma, 73116.
ee. Nikon Eclipse E600, Nikon Corporation Instruments Company, Tokyo, Japan.
ff. Nikon Coolpix 995 with Coolpix MDC adaptor, Nikon, Inc., Melville, New York, 11747.
gg. ImageJ 1.42q, Wayne Rasband, National Institutes of Health, http://rsb.info.nih.gov/ij, United States.

hh. Personnal communication with technical services, R&D Systems, Inc., Minneapolis, Minnesota, 55413.

Bibliography

1. Lazzarini L, Mader JT, Calhoun JH. Osteomyelitis in long bones.*c Am* 2004;86-A(10):2305-2318.
2. Nandi SK, Mukherjee P, Roy S, et al. Local antibiotic delivery systems for the treatment of osteomyelitis – A review. *Mater Sci Eng C Mater Biol Appl* 2009;29(8):2478-2485.
3. Miclau T, Dahners LE, Lindsey RW. In vitro pharmacokinetics of antibiotic release from locally implantable materials. *J Orthop Res* 1993;11(5):627-632.
4. McKee MD, Wild LM, Schemitsch EH, et al. The use of an antibiotic-impregnated, osteoconductive, bioabsorbable bone substitute in the treatment of infected long bone defects: early results of a prospective trial. *J Orthop Trauma* 2002;16(9):622-627.
5. Henry SL, Ostermann PA, Seligson D. The prophylactic use of antibiotic impregnated beads in open fractures. *J Trauma* 1990;30(10):1231-1238.
6. Ostermann PA, Seligson D, Henry SL. Local antibiotic therapy for severe open fractures. A review of 1085 consecutive cases. *J Bone Joint Surg Br* 1995;77(1):93-97.
7. Evans RP, Nelson CL. Gentamicin-impregnated polymethylmethacrylate beads compared with systemic antibiotic therapy in the treatment of chronic osteomyelitis. *Clin Orthop Relat Res* 1993;(295):37-42.
8. Seligson D, Mehta S, Voos K, et al. The use of antibiotic-impregnated polymethylmethacrylate beads to prevent the evolution of localized infection. *J Orthop Trauma* 1992;6(4):401-406.
9. Buchholz HW, Elson RA, Heinert K. Antibiotic-loaded acrylic cement: current concepts. *Clin Orthop Relat Res* 1984;(190):96-108.
10. Wininger DA, Fass RJ. Antibiotic-impregnated cement and beads for orthopedic infections. *Antimicrob Agents Chemother* 1996;40(12):2675-2679.
11. Klemm K. The use of antibiotic-containing bead chains in the treatment of chronic bone infections. *Clin Microbiol Infect* 2001;7(1):28-31.
12. McKee MD, Li-Bland EA, Wild LM, et al. A prospective, randomized clinical trial comparing an antibiotic-impregnated bioabsorbable bone substitute with standard antibiotic-impregnated cement beads in the treatment of chronic osteomyelitis and infected nonunion. *J Orthop Trauma* 2010;24(8):483-490.
13. Langlais F, Belot N, Ropars M, et al. Antibiotic cements in articular prostheses: current orthopaedic concepts. *Int J Antimicrob Agents* 2006;28(2):84-89.
14. Tobias KM, Schneider RK, Besser TE. Use of antimicrobial-impregnated polymethyl methacrylate. *J Am Vet Med Assoc* 1996;208(6):841-845.
15. Trostle SS, Hendrickson DA, Stone WC, et al. Use of antimicrobial-impregnated polymethyl methacrylate beads for treatment of chronic, refractory septic arthritis and osteomyelitis of the digit in a bull. *J Am Vet Med Assoc* 1996;208(3):404-407.
16. Holcombe SJ, Schneider RK, Bramlage LR, et al. Use of antibiotic-impregnated polymethyl methacrylate in horses with open or infected fractures or joints: 19 cases (1987-1995). *J Am Vet Med Assoc* 1997;211(7):889-893.

17. Butson RJ, Schramme MC, Garlick MH, et al. Treatment of intrasynovial infection with gentamicin-impregnated polymethylmethacrylate beads. *Vet Rec* 1996;138(19):460-464.

18. Trostle SS, Peavey CL, King DS, et al. Treatment of methicillin-resistant Staphylococcus epidermidis infection following repair of an ulnar fracture and humeroradial joint luxation in a horse. *J Am Vet Med Assoc* 2001;218(4):554-9, 527.

19. Hartley MP, Sanderson S. Use of antibiotic impregnated polymethylmethacrylate beads for the treatment of chronic mandibular osteomyelitis in a Bennett's wallaby (Macropus rufogriseus rufogriseus). *Aust Vet J* 2003;81(12):742-744.

20. Perry CR, Rice S, Ritterbusch JK, et al. Local administration of antibiotics with an implantable osmotic pump. *Clin Orthop Relat Res* 1985;(192):284-290.

21. Perry CR, Davenport K, Vossen MK. Local delivery of antibiotics via an implantable pump in the treatment of osteomyelitis. *Clin Orthop Relat Res* 1988;(226):222-230.

22. Garvin K, Feschuk C. Polylactide-polyglycolide antibiotic implants. *Clin Orthop Relat Res* 2005;(437):105-110.

23. Wachol-Drewek Z, Pfeiffer M, Scholl E. Comparative investigation of drug delivery of collagen implants saturated in antibiotic solutions and a sponge containing gentamicin. *Biomaterials* 1996;17(17):1733-1738.

24. Stemberger A, Grimm H, Bader F, et al. Local treatment of bone and soft tissue infections with the collagen-gentamicin sponge. *Eur J Surg Suppl* 1997;(578):17-26.

25. Mendel V, Simanowski HJ, Scholz HC, et al. Therapy with gentamicin-PMMA beads, gentamicin-collagen sponge, and cefazolin for experimental osteomyelitis due to Staphylococcus aureus in rats. *Arch Orthop Trauma Surg* 2005;125(6):363-368.

26. Shirtliff ME, Calhoun JH, Mader JT. Experimental osteomyelitis treatment with antibiotic-impregnated hydroxyapatite. *Clin Orthop Relat Res* 2002;(401):239-247.

27. Itokazu M, Ohno T, Tanemori T, et al. Antibiotic-loaded hydroxyapatite blocks in the treatment of experimental osteomyelitis in rats. *J Med Microbiol* 1997;46(9):779-783.

28. Rogers-Foy JM, Powers DL, Brosnan DA, et al. Hydroxyapatite composites designed for antibiotic drug delivery and bone reconstruction: a caprine model. *J Invest Surg* 1999;12(5):263-275.

29. Saito T, Takeuchi R, Hirakawa K, et al. Slow-releasing potential of vancomycin-loaded porous hydroxyapatite blocks implanted into MRSA osteomyelitis. *J Biomed Mater Res* 2002;63(3):245-251.

30. Joosten U, Joist A, Gosheger G, et al. Effectiveness of hydroxyapatite-vancomycin bone cement in the treatment of Staphylococcus aureus induced chronic osteomyelitis. *Biomaterials* 2005;26(25):5251-5258.

31. Shinto Y, Uchida A, Korkusuz F, et al. Calcium hydroxyapatite ceramic used as a delivery system for antibiotics. *J Bone Joint Surg Br* 1992;74(4):600-604.

32. Kundu B, Soundrapandian C, Nandi SK, et al. Development of new localized drug delivery system based on ceftriaxone-sulbactam composite drug impregnated porous hydroxyapatite: a systematic approach for in vitro and in vivo animal trial. *Pharm Res* 2010;27(8):1659-1676.

33. Dahners LE, Funderburk CH. Gentamicin-loaded plaster of Paris as a treatment of experimental osteomyelitis in rabbits. *Clin Orthop Relat Res* 1987;(219):278-282.

34. Santschi EM, McGarvey L. In vitro elution of gentamicin from Plaster of Paris beads. *Vet Surg* 2003;32(2):128-133.
35. Atilla A, Boothe HW, Tollett M, et al. In vitro elution of amikacin and vancomycin from impregnated plaster of Paris beads. *Vet Surg* 2010;39(6):715-721.
36. Aimin C, Chunlin H, Juliang B, et al. Antibiotic loaded chitosan bar. An in vitro, in vivo study of a possible treatment for osteomyelitis. *Clin Orthop Relat Res* 1999;(366):239-247.
37. Orhan Z, Cevher E, Mülazimoğlu L, et al. The preparation of ciprofloxacin hydrochloride-loaded chitosan and pectin microspheres: their evaluation in an animal osteomyelitis model. *J Bone Joint Surg Br* 2006;88(2):270-275.
38. Cevher E, Orhan Z, Sensoy D, et al. Sodium fusidate-poly(D,L-lactide-co-glycolide) microspheres: preparation, characterisation and in vivo evaluation of their effectiveness in the treatment of chronic osteomyelitis. *J Microencapsul* 2007;24(6):577-595.
39. Orhan Z, Cevher E, Yildiz A, et al. Biodegradable microspherical implants containing teicoplanin for the treatment of methicillin-resistant Staphylococcus aureus osteomyelitis. *Arch Orthop Trauma Surg* 2010;(130):135-142.
40. Garvin KL, Miyano JA, Robinson D, et al. Polylactide/polyglycolide antibiotic implants in the treatment of osteomyelitis. A canine model. *J Bone Joint Surg Am* 1994;76(10):1500-1506.
41. Wang G, Liu SJ, Ueng SW, et al. The release of cefazolin and gentamicin from biodegradable PLA/PGA beads. *Int J Pharm* 2004;273(1-2):203-212.
42. Naraharisetti PK, Guan Lee HC, Fu YC, et al. In vitro and in vivo release of gentamicin from biodegradable discs. *J Biomed Mater Res B Appl Biomater* 2006;77(2):329-337.
43. Chen L, Wang H, Wang J, et al. Ofloxacin-delivery system of a polyanhydride and polylactide blend used in the treatment of bone infection. *J Biomed Mater Res B Appl Biomater* 2007;83(2):589-595.
44. Virto MR, Elorza B, Torrado S, et al. Improvement of gentamicin poly(D,L-lactic-co-glycolic acid) microspheres for treatment of osteomyelitis induced by orthopedic procedures. *Biomaterials* 2007;28(5):877-885.
45. Ueng SW, Yuan LJ, Lee N, et al. In vivo study of hot compressing molded 50:50 poly (DL-lactide-co-glycolide) antibiotic beads in rabbits. *J Orthop Res* 2002;20(4):654-661.
46. Liu SS, Ueng S, Lin SS, et al. In vivo release of vancomycin from biodegradable beads. *J Biomed Mater Res* 2002;63(6):807-813.
47. Liu SS, Chi P, Lin SS, et al. Novel solvent-free fabrication of biodegradable poly-lactic-glycolic acid (PLGA) capsules for antibiotics and rhBMP-2 delivery. *Int J Pharm* 2007;330(1-2):45-53.
48. Calhoun JH, Mader JT. Treatment of osteomyelitis with a biodegradable antibiotic implant. *Clin Orthop Relat Res* 1997;(341):206-214.
49. Mader JT, Calhoun J, Cobos J. In vitro evaluation of antibiotic diffusion from antibiotic-impregnated biodegradable beads and polymethylmethacrylate beads. *Antimicrob Agents Chemother* 1997;41(2):415-418.
50. Ambrose CG, Gogola GR, Clyburn TA, et al. Antibiotic microspheres: preliminary testing for potential treatment of osteomyelitis. *Clin Orthop Relat Res* 2003;(415):279-285.

51. Ambrose CG, Clyburn TA, Louden K, et al. Effective treatment of osteomyelitis with biodegradable microspheres in a rabbit model. *Clin Orthop Relat Res* 2004;(421):293-299.
52. Changez M, Koul V, Krishna B, et al. Studies on biodegradation and release of gentamicin sulphate from interpenetrating network hydrogels based on poly(acrylic acid) and gelatin: in vitro and in vivo. *Biomaterials* 2004;25(1):139-146.
53. Changez M, Koul V, Dinda AK. Efficacy of antibiotics-loaded interpenetrating network (IPNs) hydrogel based on poly(acrylic acid) and gelatin for treatment of experimental osteomyelitis: in vivo study. *Biomaterials* 2005;26(14):2095-2104.
54. Rutledge B, Huyette D, Day D, et al. Treatment of osteomyelitis with local antibiotics delivered via bioabsorbable polymer. *Clin Orthop Relat Res* 2003;(411):280-287.
55. Li LC, Deng J, Stephens D. Polyanhydride implant for antibiotic delivery--from the bench to the clinic. *Adv Drug Deliv Rev* 2002;54(7):963-986.
56. Krasko MY, Golenser J, Nyska A, et al. Gentamicin extended release from an injectable polymeric implant. *J Control Release* 2007;117(1):90-96.
57. Yenice I, Caliş S, Kaş H, et al. Biodegradable implantable teicoplanin beads for the treatment of bone infections. *Int J Pharm* 2002;242(1-2):271-275.
58. Yenice I, Caliş S, Atilla B, et al. In vitro/in vivo evaluation of the efficiency of teicoplanin-loaded biodegradable microparticles formulated for implantation to infected bone defects. *J Microencapsul* 2003;20(6):705-717.
59. Hendricks KJ, Lane D, Burd TA, et al. Elution characteristics of tobramycin from polycaprolactone in a rabbit model. *Clin Orthop Relat Res* 2001;(392):418-426.
60. Korkusuz F, Korkusuz P, Ekşioĝlu F, et al. In vivo response to biodegradable controlled antibiotic release systems. *J Biomed Mater Res* 2001;55(2):217-228.
61. Dounis E, Korakis T, Anastasiadis A, et al. Sustained release of fleroxacin in vitro from lactic acid polymer. *Bull Hosp Jt Dis* 1996;55(1):16-19.
62. Kanellakopoulou K, Kolia M, Anastassiadis A, et al. Lactic acid polymers as biodegradable carriers of fluoroquinolones: an in vitro study. *Antimicrob Agents Chemother* 1999;43(3):714-716.
63. Schierholz JM, Steinhauser H, Rump AF, et al. Controlled release of antibiotics from biomedical polyurethanes: morphological and structural features. *Biomaterials* 1997;18(12):839-844.
64. Itokazu M, Yamamoto K, Yang WY, et al. The sustained release of antibiotic from freeze-dried fibrin-antibiotic compound and efficacies in a rat model of osteomyelitis. *Infection* 1997;25(6):359-363.
65. Tsourvakas S, Hatzigrigoris P, Tsibinos A, et al. Pharmacokinetic study of fibrin clot-ciprofloxacin complex: an in vitro and in vivo experimental investigation. *Arch Orthop Trauma Surg* 1995;114(5):295-297.
66. Mader JT, Stevens CM, Stevens JH, et al. Treatment of experimental osteomyelitis with a fibrin sealant antibiotic implant. *Clin Orthop Relat Res* 2002;(403):58-72.
67. Li XD, Hu YY. The treatment of osteomyelitis with gentamicin-reconstituted bone xenograft-composite. *J Bone Joint Surg Br* 2001;83(7):1063-1068.

68. McLaren AC, McLaren SG, Nelson CL, et al. The effect of sampling method on the elution of tobramycin from calcium sulfate. *Clin Orthop Relat Res* 2002;(403):54-57.

69. Nelson CL, McLaren SG, Skinner RA, et al. The treatment of experimental osteomyelitis by surgical debridement and the implantation of calcium sulfate tobramycin pellets. *J Orthop Res* 2002;20(4):643-647.

70. Webb N, McCanless J, Courtney H, et al. Daptomycin eluted from calcium sulfate appears effective against Staphylococcus. *Clin Orthop* 2008;466(6):1383-1387.

71. Lambotte JC, Thomazeau H, Cathelineau G, et al. [Tricalcium phosphate, an antibiotic carrier: a study focused on experimental osteomyelitis in rabbits]. *Chirurgie* 1998;123(6):572-579.

72. Matsuno H, Yudoh K, Hashimoto M, et al. Antibiotic-containing hyaluronic acid gel as an antibacterial carrier: Usefulness of sponge and film-formed HA gel in deep infection. *J Orthop Res* 2006;24(3):321-326.

73. Ouédraogo M, Semdé R, Somé IT, et al. Monoolein-water liquid crystalline gels of gentamicin as bioresorbable implants for the local treatment of chronic osteomyelitis: in vitro characterization. *Drug Dev Ind Pharm* 2008;34(7):753-760.

74. Rauschmann MA, Wichelhaus TA, Stirnal V, et al. Nanocrystalline hydroxyapatite and calcium sulphate as biodegradable composite carrier material for local delivery of antibiotics in bone infections. *Biomaterials* 2005;26(15):2677-2684.

75. Simchi A, Tamjid E, Pishbin F, et al. Recent progress in inorganic and composite coatings with bactericidal capability for orthopaedic applications. *Nanomedicine* 2010; In press (doi:10.1016/j.nano.2010.10.005).

76. Liu H, Zhang L, Shi P, et al. Hydroxyapatite/polyurethane scaffold incorporated with drug-loaded ethyl cellulose microspheres for bone regeneration. *J Biomed Mater Res B Appl Biomater* 2010;95(1):36-46.

77. Anand A, Pundir R, Pandian CS, et al. Cefoperazone sodium impregnated polycaprolactone composite implant for osteomyelitis. *Indian J Pharm Sci* 2009;71(4):377-381.

78. Jia WT, Zhang X, Zhang CQ, et al. Elution characteristics of teicoplanin-loaded biodegradable borate glass/chitosan composite. *Int J Pharm* 2010;387(1-2):184-186.

79. Porter JR, Ruckh TT, Popat KC. Bone tissue engineering: a review in bone biomimetics and drug delivery strategies. *Biotechnol Prog* 2009;25(6):1539-1560.

80. Nade S. The replacement of broken, missing, and diseased bone. In: *Bone in Clinical Orthopedics.* 2nd ed. Dubendorf: AO Publishing, 2002;379-409.

81. Fitch R, Kerwin S, Newman-Gage H, et al. Bone autografts and allografts in dogs. *Compend Contin Educ Pract Vet* 1997;19(5):558-578.

82. Dorea HC, McLaughlin RM, Cantwell HD, et al. Evaluation of healing in feline femoral defects filled with cancellous autograft, cancellous allograft or Bioglass. *Vet Comp Orthop Traumatol* 2005;18(3):157-168.

83. Chase SW, Herndon CH. The fate of autogenous and homogenous bone grafts. *J Bone Joint Surg Am* 1955;37-A(4):809-841.

84. Malizos KN, Dailiana ZH, Innocenti M, et al. Vascularized bone grafts for upper limb reconstruction: defects at the distal radius, wrist, and hand. *J Hand Surg Am* 2010;35(10):1710-1718.

85. Schwartz AJ, Jones NF, Seeger LL, et al. Chronic sclerosing osteomyelitis treated with wide resection and vascularized fibular autograft: a case report. *Am J Orthop* 2010;39(3):E28-E32.

86. Vertenten G, Gasthuys F, Cornelissen M, et al. Enhancing bone healing and regeneration: present and future perspectives in veterinary orthopaedics. *Vet Comp Orthop Traumatol* 2010;23(3):153-162.

87. Nakase T, Nomura S, Yoshikawa H, et al. Transient and localized expression of bone morphogenetic protein 4 messenger RNA during fracture healing. *J Bone Miner Res* 1994;9(5):651-659.

88. Schmitt JM, Hwang K, Winn SR, et al. Bone morphogenetic proteins: an update on basic biology and clinical relevance. *J Orthop Res* 1999;17(2):269-278.

89. Yoshimura Y, Nomura S, Kawasaki S, et al. Colocalization of noggin and bone morphogenetic protein-4 during fracture healing. *J Bone Miner Res* 2001;16(5):876-884.

90. Cheng H, Jiang W, Phillips FM, et al. Osteogenic activity of the fourteen types of human bone morphogenetic proteins (BMPs). *J Bone Joint Surg Am volume* 2003;85-A(8):1544-1552.

91. Hanamura H, Higuchi Y, Nakagawa M, et al. Solubilized bone morphogenetic protein (BMP) from mouse osteosarcoma and rat demineralized bone matrix. *Clin Orthop Relat Res* 1980;(148):281-290.

92. Liao JC, Tzeng ST, Keorochana G, et al. Enhancement of recombinant human BMP-7 bone formation with bmp binding peptide in a rodent femoral defect model. *J Orthop Res* 2010; In press (doi: 10.1002/jor.21252).

93. McKay WF, Peckham SM, Badura JM. A comprehensive clinical review of recombinant human bone morphogenetic protein-2 (INFUSE Bone Graft). *Int Orthop* 2007;31(6):729-734.

94. Govender S, Csimma C, Genant HK, et al. Recombinant human bone morphogenetic protein-2 for treatment of open tibial fractures: a prospective, controlled, randomized study of four hundred and fifty patients. *J Bone Joint Surg Am* 2002;84-A(12):2123-2134.

95. Chen X, Schmidt AH, Mahjouri S, et al. Union of a chronically infected internally stabilized segmental defect in the rat femur after debridement and application of rhBMP-2 and systemic antibiotic. *J Orthop Trauma* 2007;21(10):693-700.

96. Chen X, Kidder LS, Lew WD. Osteogenic protein-1 induced bone formation in an infected segmental defect in the rat femur. *J Orthop Res* 2002;20(1):142-150.

97. Worlock P, Slack R, Harvey L, et al. The prevention of infection in open fractures: an experimental study of the effect of fracture stability. *Injury* 1994;25(1):31-38.

98. Anderson DE, Desrochers A. Musculoskeletal Examination in Cattle. In: Fubini SL, Ducharme NG, ed. *Farm Animal Surgery.* St. Louis: Saunders Elsevier, 2004;283-290.

99. Kao ST, Scott DD. A review of bone substitutes. *Oral Maxillofac Surg Clin North Am* 2007;19(4):513-21, vi.

100. Niehaus AJ, Anderson DE, Samii VF, et al. Effects of orthopedic implants with a polycaprolactone polymer coating containing bone morphogenetic protein-2 on osseointegration in bones of sheep. *Am J Vet Res* 2009;70(11):1416-1425.

101. Ignjatović NL, Ninkov P, Sabetrasekh R, et al. A novel nano drug delivery system based on tigecycline-loaded calciumphosphate coated with poly-DL-lactide-co-glycolide. *J Mater Sci Mater Med* 2010;21(1):231-239.

102. Agrawal CM, Best J, Heckman JD, et al. Protein release kinetics of a biodegradable implant for fracture non-unions. *Biomaterials* 1995;16(16):1255-1260.

103. Lee JW, Kang KS, Lee SH, et al. Bone regeneration using a microstereolithography-produced customized poly(propylene fumarate)/diethyl fumarate photopolymer 3D scaffold incorporating BMP-2 loaded PLGA microspheres. *Biomaterials* 2011;32(3):744-752.

104. Zande MV, Walboomers XF, Olalde B, et al. Effect of nanotubes and apatite on growth factor release from PLLA scaffolds. *J Tissue Eng Regen Med* 2010;In press (doi: 10.1002/term.339).

105. Bae IH, Yun KD, Kim HS, et al. Anodic oxidized nanotubular titanium implants enhance bone morphogenetic protein-2 delivery. *J Biomed Mater Res B Appl Biomater* 2010;93(2):484-491.

106. Macdonald ML, Samuel RE, Shah NJ, et al. Tissue integration of growth factor-eluting layer-by-layer polyelectrolyte multilayer coated implants. *Biomaterials* 2011;32(5):1446-1453.

107. Soundrapandian C, Sa B, Datta S. Organic-inorganic composites for bone drug delivery. *AAPS PharmSciTech* 2009;10(4):1158-1171.

108. Issa JP, Bentley MV, Iyomasa MM, et al. Sustained release carriers used to delivery bone morphogenetic proteins in the bone healing process. *Anat Histol Embryol* 2008;37(3):181-187.

109. Puleo DA. Dependence of mesenchymal cell responses on duration of exposure to bone morphogenetic protein-2 in vitro. *J Cell Physiol* 1997;173(1):93-101.

110. Puleo DA, Huh WW, Duggirala SS, et al. In vitro cellular responses to bioerodible particles loaded with recombinant human bone morphogenetic protein-2. *J Biomed Mater Res* 1998;41(1):104-110.

111. Blokhuis TJ. Formulations and delivery vehicles for bone morphogenetic proteins: latest advances and future directions. *Injury* 2009;40 Suppl 3:S8-11.

112. Galanakis N, Giamarellou H, Moussas T, et al. Chronic osteomyelitis caused by multi-resistant Gram-negative bacteria: evaluation of treatment with newer quinolones after prolonged follow-up. *J Antimicrob Chemother* 1997;39(2):241-246.

113. Rissing JP. Antimicrobial therapy for chronic osteomyelitis in adults: role of the quinolones. *Clin Infect Dis* 1997;25(6):1327-1333.

114. Lazzarini L, Lipsky B, Mader J. Antibiotic treatment of osteomyelitis: what have we learned from 30 years of clinical trials? *Int J Infect Dis* 2005;9(3):127-138.

115. Kuli B, de Barbeyrac B, Dauchy FA, et al. In vitro activities of daptomycin, tigecycline, linezolid and eight other antibiotics, alone and in combination, against 41 Staphylococcus spp. clinical isolates from bone and joint infections. *Int J Antimicrob Agents* 2009;33(5):491-493.

116. Gautier H, Plumecocq A, Amador G, et al. In Vitro Characterization of Calcium Phosphate Biomaterial Loaded with Linezolid for Osseous Bone Defect Implantation. *J Biomater Appl* 2010;In press (doi: 10.1177/0885328210381535).

117. Noskin GA. Tigecycline: a new glycylcycline for treatment of serious infections. *Clin Infect Dis* 2005;41 Suppl 5:S303-S314.

118. Gales AC, Jones RN, Andrade SS, et al. In vitro activity of tigecycline, a new glycylcycline, tested against 1,326 clinical bacterial strains isolated from Latin America. *Braz J Infect Dis* 2005;9(5):348-356.

119. Yin LY, Lazzarini L, Li F, et al. Comparative evaluation of tigecycline and vancomycin, with and without rifampicin, in the treatment of methicillin-resistant Staphylococcus aureus experimental osteomyelitis in a rabbit model. *J Antimicrob Chemother* 2005;55(6):995-1002.

120. Dowling PM. Aminoglycosides. In: Giguère S, Prescott JF, Baggot JD, Walker RD, Dowling PM, eds. *Antimicrobial Therapy in Veterinary Medicine.* 4th ed. Ames, Iowa: Blackwell Publishing, 2006;207-229.

121. Pilloud M. [Antibiotics and chemotherapy--from research to practice. VI. Remarks addressed to practitioners concerning aminoglucoside characteristics]. *Schweiz Arch Tierheilkd* 1983;125(5):301-315.

122. Miclau T, Edin ML, Lester GE, et al. Bone toxicity of locally applied aminoglycosides. *J Orthop Trauma* 1995;9(5):401-406.

123. Zalavras CG, Patzakis MJ, Holtom P. Local antibiotic therapy in the treatment of open fractures and osteomyelitis. *Clin Orthop Relat Res* 2004;(427):86-93.

124. Chopra I. Genetic and biochemical basis of tetracycline resistance. *J Antimicrob Chemother* 1986;18 Suppl C:51-56.

125. Petersen PJ, Jacobus NV, Weiss WJ, et al. In vitro and in vivo antibacterial activities of a novel glycylcycline, the 9-t-butylglycylamido derivative of minocycline (GAR-936). *Antimicrob Agents Chemother* 1999;43(4):738-744.

126. Fluit AC, Florijn A, Verhoef J, et al. Presence of tetracycline resistance determinants and susceptibility to tigecycline and minocycline. *Antimicrob Agents Chemother* 2005;49(4):1636-1638.

127. Pina C, Ferraz MP, Coelho MJ. The effects of tigecycline on human osteoblasts in vitro. Revista da Faculdade de Ciências da Saude 2008;5:146-152 (http://hdl.handle.net/10284/941).

128. Miclau T, Edin ML, Lester GE, et al. Gentamicin wound irrigation, in 61st annual meeting of the AAOS 1994.

129. Antoci V Jr, Adams CS, Hickok NJ, et al. Antibiotics for local delivery systems cause skeletal cell toxicity in vitro. *Clin Orthop Relat Res* 2007;462:200-206.

130. Freeman CD, Nicolau DP, Belliveau PP, et al. Once-daily dosing of aminoglycosides: review and recommendations for clinical practice. *J Antimicrob Chemother* 1997;39(6):677-686.

131. Powell SH, Thompson WL, Luthe MA, et al. Once-daily vs. continuous aminoglycoside dosing: efficacy and toxicity in animal and clinical studies of gentamicin, netilmicin, and tobramycin. *J Infect Dis* 1983;147(5):918-932.

132. Bucki EP, Giguère S, Macpherson M, et al. Pharmacokinetics of once-daily amikacin in healthy foals and therapeutic drug monitoring in hospitalized equine neonates. *J Vet Intern Med* 2004;18(5):728-733.

133. Mattie H, Craig WA, Pechère JC. Determinants of efficacy and toxicity of aminoglycosides. *J Antimicrob Chemother* 1989;24(3):281-293.

134. Walenkamp GH, Vree TB, van Rens TJ. Gentamicin-PMMA beads. Pharmacokinetic and nephrotoxicological study. *Clin Orthop Relat Res* 1986;(205):171-183.

135. Tabas JA, Zasloff M, Wasmuth JJ, et al. Bone morphogenetic protein: chromosomal localization of human genes for BMP1, BMP2A, and BMP3. *Genomics* 1991;9(2):283-289.

136. Fang X, Xu H, Zhang C, et al. Polymorphisms in BMP-2 gene and their associations with growth traits in goats. *Genes Genomics* 2010;32(1):29-35.

137. Poynton AR, Lane JM. Safety profile for the clinical use of bone morphogenetic proteins in the spine. *Spine* 2002;27(16 Suppl 1):S40-S48.

138. Kawaguchi AT, Reddi AH, Olson SA, et al. Are recombinant human bone morphogenetic protein-7 and tobramycin compatible? An experiment in rats. *J Orthop Trauma* 2004;18(4):225-232.

139. Suzuki A, Terai H, Toyoda H, et al. A biodegradable delivery system for antibiotics and recombinant human bone morphogenetic protein-2: A potential treatment for infected bone defects. *J Orthop Res* 2006;24(3):327-332.

140. Glatt V, Kwong FN, Park K, et al. Ability of recombinant human bone morphogenetic protein 2 to enhance bone healing in the presence of tobramycin: evaluation in a rat segmental defect model. *J Orthop Trauma* 2009;23(10):693-701.

141. An YH FR. Animal selections in orthopaedic research. In: An YH FR, ed. *Animal Models in Orthopaedic Research.* Boca Raton, FL: CRC Press LLC, 1999;39-57.

142. Pearce AI, Richards RG, Milz S, et al. Animal models for implant biomaterial research in bone: a review. *Eur Cell Mater* 2007;13:1-10.

143. Spaargaren DH. Metabolic rate and body size: a new view on the 'surface law' for basic metabolic rate. *Acta Biotheor* 1994;42(4):263-269.

144. Anderson ML, Dhert WJ, de Bruijn JD, et al. Critical size defect in the goat's os ilium. A model to evaluate bone grafts and substitutes. *Clin Orthop Relat Res* 1999;(364):231-239.

145. Dai KR, Xu XL, Tang TT, et al. Repairing of goat tibial bone defects with BMP-2 gene-modified tissue-engineered bone. *Calcif Tissue Int* 2005;77(1):55-61.

146. Goodell JA, Flick AB, Hebert JC, et al. Preparation and release characteristics of tobramycin-impregnated polymethylmethacrylate beads. *Am J Hosp Pharm* 1986;43(6):1454-1461.

147. Nelson CL, Griffin FM, Harrison BH, et al. In vitro elution characteristics of commercially and noncommercially prepared antibiotic PMMA beads. *Clin Orthop Relat Res* 1992;(284):303-309.

Appendix A - Supplementary Tables

Table A.1 I*n Vitro* Elution Data of rhBMP-2, Tigecycline, and Tobramycin from the Novel Polymeric Bone Matrix, Days 0-30

Time (days)	rhBMP-2 impregnated matrix	Antimicrobials impregnated matrix		rhBMP-2 and antimicrobials impregnated matrix		
	rhBMP-2 [C] (pg/ml)	Tigecycline [C] (ng/ml)	Tobramycin [C] (ng/ml)	rhBMP-2 [C] (pg/ml)	Tigecycline [C] (ng/ml)	Tobramycin [C] (ng/ml)
1	922,880	49800	125000	.	.	.
2	916,480	18500	28200	302,080	9960	.
3	532,480	14600	5920	145,280	6950	.
4	422,080	9650	1550	178,880	7890	859
5	326,080	5960	891	153,280	4690	347
6	276,480	4090	429	113,280	5700	.
8	247,680	3280	267	143,680	5280	238
10	156,480	1080	.	124,480	3170	117
13	298,880	1210	70.8	159,680	2890	109
15	450,880	818	71.2	121,280	2010	46.8
17	193,280	797	38.4	108,480	1090	26.7
21	199,680	475	32.8	119,680	1410	27.2
25	202,880	379	51.5	121,280	811	40.1
28	167,680	390	22.7	100,480	349	11.4
30	130,880	248	23.4	116,480	360	6.1

Table A.2 Initial Hind Limb Lameness Scores for Goats in Group 1 (C), Days 0-17

Time	Goat 32 Left	Goat 32 Right	Goat 35 Left	Goat 35 Right	Goat 38 Left	Goat 38 Right	Goat 43 Left	Goat 43 Right
D0 / AM	0	0	0	0	0	0	0	0
D0 / PM	0	0	3	0	0	0	0	0
D1 / AM	0	0	1	0	0	0	1	0
D1 / PM	0	0	1	0	0	0	0	0
D2 / AM	0	0	0	0	1	0	0	0
D2 / PM	0	0	.	.	.	.	.	.
D3 / AM	1	0	1	0	0	0	0	0
D3 / PM	1	0	1	0	0	0	0	0
D4 / AM	2	0	2	0	1	0	.	.
D4 / PM	1	0	1	0	0	0	1	0
D5 / AM	0	0	1	0	0	0	0	0
D5 / PM	0	0	0	0	0	0	0	0
D6 / AM	0	0	1	0	0	0	0	0
D6 / PM	0	0	1	0	0	0	0	0
D7 / AM	0	0	1	0	0	0	0	0
D7 / PM	.	.	1	0	0	0	0	0
D8 / AM	0	0	1	0	0	1	0	0
D8 / PM	.	.	.	.	0	1	.	.
D9 / AM	0	0	0	0	0	0	0	0
D9 / PM	.	.	0	0	0	0	0	0
D10 / AM	.	.	0	0	0	0	0	0
D10 / PM	0	0	0	0	0	1	.	.
D11 / AM	0	0	0	0	0	0	0	0
D11 / PM	0	0	0	0	0	0	.	.
D12 / AM	0	0	1	1	0	0	0	0
D12 / PM	0	0	1	1	0	0	0	0
D13 / AM	0	0	0	0	0	0	.	.
D13 / PM	.	.	0	0	0	0	0	0
D14 / AM	0	0	0	0	0	0	0	0
D14 / PM	0	0	0	0	.	.	0	0
D15 / AM	0	0	0	0	0	0	.	.
D15 / PM	0	0	.	.	.	.	.	.
D16 / AM	0	0	0	0	0	0	.	.
D16 / PM	.	.	.	.	.	.	.	.
D17 / AM	.	.	0	0	0	0	.	.
D17 / PM	.	.	.	.	.	.	.	.

Legend: D = day; AM = morning evaluation; PM = evening evaluation; score 0 = normal gait; score 1 = mild lameness; score 2 = moderate lameness; score 3 = severe lameness; score 4 = catastrophic lameness. Please note that the initial lameness scores are presented here, before recoding them into code 0 = normal gait (initial score of 0) and code 1 = lameness score ≥ 1.

Table A.3 Initial Hind Limb Lameness Scores for Goats in Group 2 (M), Days 0-17

Time	Goat 42 Left	Goat 42 Right	Goat 44 Left	Goat 44 Right	Goat 47 Left	Goat 47 Right	Goat 48 Left	Goat 48 Right
D0 / AM	0	0	0	0	0	0	0	0
D0 / PM	1	2	0	0	0	2	0	1
D1 / AM	0	0	1	0	3	0	0	0
D1 / PM	0	0	.	.	2	0	0	0
D2 / AM	0	0	0	0	1	0	1	0
D2 / PM	.	.	0	0	1	0	1	0
D3 / AM	0	1	.	.	.	.	.	.
D3 / PM	0	1	0	0	3	0	0	1
D4 / AM	.	.	0	0	2	0	1	0
D4 / PM	0	0	0	0	3	0	0	1
D5 / AM	0	0	0	0	3	0	0	0
D5 / PM	0	0	0	0	2	0	0	0
D6 / AM	0	1	0	0	2	0	0	0
D6 / PM	0	0	0	0	3	0	0	0
D7 / AM	0	0	0	0	2	0	0	0
D7 / PM	0	0	.	.	.	.	.	.
D8 / AM	0	0	0	0	1	0	0	0
D8 / PM	.	.	.	.	.	.	.	.
D9 / AM	0	0	0	0	0	0	0	0
D9 / PM	0	0	.	.	.	.	.	.
D10 / AM	0	0	.	.	.	.	.	.
D10 / PM	.	.	0	0	0	0	0	0
D11 / AM	0	0	0	0	0	0	0	0
D11 / PM	.	.	0	0	0	0	0	0
D12 / AM	0	0	0	0	0	0	0	1
D12 / PM	0	0	0	0	0	0	0	0
D13 / AM	.	.	0	0	0	0	0	1
D13 / PM	0	0	.	.	.	.	.	.
D14 / AM	0	0	0	0	0	0	0	1
D14 / PM	0	0	0	0	0	0	0	1
D15 / AM	0	0	0	0	0	0	0	1
D15 / PM	0	0	0	0	0	0	0	0
D16 / AM	0	0	0	0	0	0	0	0
D16 / PM	0	0	.	.	.	.	.	.
D17 / AM	0	0	.	.	0	0	.	.
D17 / PM	.	.	.	.	.	.	.	.

Legend: D = day; AM = morning evaluation; PM = evening evaluation; score 0 = normal gait; score 1 = mild lameness; score 2 = moderate lameness; score 3 = severe lameness; score 4 = catastrophic lameness. Please note that the initial lameness scores are presented here, before recoding them into code 0 = normal gait (initial score of 0) and code 1 = lameness score ≥ 1.

Table A.4 Initial Hind Limb Lameness Scores for Goats in Group 3 (MAb), Days 0-17

Time	Goat 39		Goat 40		Goat 41		Goat 45	
	Left	Right	Left	Right	Left	Right	Left	Right
D0 / AM	0	0	0	0	0	0	0	0
D0 / PM	1	0	1	2	2	2	0	1
D1 / AM	1	0	0	1	2	2	0	1
D1 / PM	0	0	1	2	1	1	0	0
D2 / AM	0	0	0	1	2	0	0	0
D2 / PM	.	.	.	.	.	.	0	0
D3 / AM	0	3	0	3	0	0	.	.
D3 / PM	0	2	0	2	0	0	0	0
D4 / AM	.	.	.	.	.	.	0	0
D4 / PM	0	0	0	2	0	0	0	0
D5 / AM	0	0	0	1	0	0	0	0
D5 / PM	0	0	0	2	0	0	0	0
D6 / AM	0	0	0	1	0	0	0	0
D6 / PM	0	1	0	3	0	0	0	0
D7 / AM	0	1	0	2	0	0	0	0
D7 / PM	0	0	0	2	0	0	.	.
D8 / AM	0	1	0	1	0	0	0	0
D8 / PM	.	.	.	.	.	.	.	.
D9 / AM	0	0	0	0	0	0	0	0
D9 / PM	0	0	0	0	0	0	.	.
D10 / AM	0	0	0	0	0	0	.	.
D10 / PM	.	.	.	.	.	.	0	0
D11 / AM	0	0	0	0	0	0	0	0
D11 / PM	.	.	.	.	.	.	0	0
D12 / AM	0	0	0	0	0	0	0	0
D12 / PM	0	1	0	0	0	0	0	0
D13 / AM	.	.	.	.	.	.	0	0
D13 / PM	0	1	0	0	0	0	.	.
D14 / AM	1	0	0	0	0	0	0	0
D14 / PM	.	.	.	.	0	0	0	0
D15 / AM	0	0	0	0	0	0	0	0
D15 / PM	0	0	0	0	0	0	0	0
D16 / AM	0	0	0	0	0	0	0	0
D16 / PM	0	1	0	0	0	0	.	.
D17 / AM	0	0	0	0	0	0	.	.
D17 / PM	.	.	.	.	.	.	.	.

Legend: D = day; AM = morning evaluation; PM = evening evaluation; score 0 = normal gait; score 1 = mild lameness; score 2 = moderate lameness; score 3 = severe lameness; score 4 = catastrophic lameness. Please note that the initial lameness scores are presented here, before recoding them into code 0 = normal gait (initial score of 0) and code 1 = lameness score ≥ 1.

Table A.5 Initial Hind Limb Lameness Scores for Goats in Group 4 (MBMP), Days 0-17

Time	Goat 27 Left	Goat 27 Right	Goat 29 Left	Goat 29 Right	Goat 33 Left	Goat 33 Right	Goat 36 Left	Goat 36 Right
D0 / AM	0	0	0	0	0	0	0	0
D0 / PM	1	0	0	0	0	1	0	0
D1 / AM	0	1	0	0	1	0	0	1
D1 / PM	0	1	1	0	1	0	1	0
D2 / AM	0	1	0	0	0	2	0	0
D2 / PM	.	.	.	.	0	1	.	.
D3 / AM	0	1	0	1	0	2	0	0
D3 / PM	.	.	.	.	0	2	0	2
D4 / AM	1	1	0	0	0	2	0	2
D4 / PM	0	2	0	0	0	2	0	2
D5 / AM	0	0	0	0	0	0	0	2
D5 / PM	0	1	0	1	0	1	2	0
D6 / AM	0	1	0	0	1	0	0	2
D6 / PM	0	0	0	1	0	2	0	1
D7 / AM	0	1	0	1	0	1	0	1
D7 / PM	1	0	0	1	0	1	0	1
D8 / AM	0	1	1	0	0	0	0	1
D8 / PM	.	.	.	.	0	0	0	1
D9 / AM	0	0	0	0	0	0	0	0
D9 / PM	0	0	0	0	0	0	0	0
D10 / AM	0	0	0	0	0	0	0	0
D10 / PM	0	0	0	0	0	0	0	0
D11 / AM	0	0	.	.	0	0	0	0
D11 / PM	0	0	0	0	0	0	0	0
D12 / AM	0	0	1	0	0	0	0	0
D12 / PM	0	0	0	0	0	0	0	0
D13 / AM	0	0	0	0	0	0	0	0
D13 / PM	0	0	0	0	0	0	0	0
D14 / AM	0	0	0	0	0	0	0	0
D14 / PM	0	0	0	0	0	0	0	0
D15 / AM	0	0	0	0	0	0	0	0
D15 / PM	.	.	.	.	.	.	.	.
D16 / AM	0	0	0	0	0	0	0	0
D16 / PM	.	.	.	.	.	.	.	.
D17 / AM	0	0	0	0	0	0	0	0
D17 / PM	.	.	.	.	.	.	.	.

Legend: D = day; AM = morning evaluation; PM = evening evaluation; score 0 = normal gait; score 1 = mild lameness; score 2 = moderate lameness; score 3 = severe lameness; score 4 = catastrophic lameness. Please note that the initial lameness scores are presented here, before recoding them into code 0 = normal gait (initial score of 0) and code 1 = lameness score ≥ 1.

Table A.6 Initial Hind Limb Lameness Scores for Goats in Group 5 (MAbBMP), Days 0-17

Time	Goat 18		Goat 30		Goat 34		Goat 37	
	Left	Right	Left	Right	Left	Right	Left	Right
D0 / AM	0	0	0	0	0	0	0	0
D0 / PM	1	0	0	0	1	0	0	0
D1 / AM	1	0	0	0	0	0	1	0
D1 / PM	0	1	1	0	0	0	0	0
D2 / AM	1	1	1	0	0	1	0	1
D2 / PM	.	.	.	.	0	0	.	.
D3 / AM	0	1	0	1	2	0	0	1
D3 / PM	.	.	.	.	0	0	0	0
D4 / AM	0	0	0	0	0	1	0	0
D4 / PM	1	0	0	0	0	1	0	0
D5 / AM	0	0	0	1	1	1	0	0
D5 / PM	1	1	0	1	0	1	0	0
D6 / AM	0	0	0	0	0	0	0	0
D6 / PM	0	0	1	0	0	1	0	1
D7 / AM	0	0	1	0	0	1	0	1
D7 / PM	0	1	0	1	0	0	0	0
D8 / AM	0	0	1	0	0	1	1	0
D8 / PM	0	0	1	0	0	1	1	0
D9 / AM	0	0	1	0	1	0	1	0
D9 / PM	0	0	.	.	1	0	1	0
D10 / AM	0	0	0	0	0	0	1	0
D10 / PM	0	0	0	0	0	0	1	0
D11 / AM	.	.	0	0	0	0	0	0
D11 / PM	1	0	0	0	0	0	1	0
D12 / AM	1	0	1	0	0	0	0	0
D12 / PM	1	0	0	0	1	0	0	0
D13 / AM	1	0	1	0	0	0	0	0
D13 / PM	0	0	0	0	0	0	0	0
D14 / AM	0	0	0	0	0	0	0	0
D14 / PM	0	0	0	0	0	0	.	.
D15 / AM	0	0	0	0	0	0	0	0
D15 / PM	.	.	.	.	.	.	.	.
D16 / AM	0	0	0	0	0	0	0	0
D16 / PM	.	.	.	.	.	.	.	.
D17 / AM	0	0	0	0	0	0	0	0
D17 / PM	.	.	.	.	.	.	.	.

Legend: D = day; AM = morning evaluation; PM = evening evaluation; score 0 = normal gait; score 1 = mild lameness; score 2 = moderate lameness; score 3 = severe lameness; score 4 = catastrophic lameness. Please note that the initial lameness scores are presented here, before recoding them into code 0 = normal gait (initial score of 0) and code 1 = lameness score ≥ 1.

Table A.7 Recoded Radiographic Scores of Healing Tibial Bone Defects in all Goats, Day 30

Goat	Endosteal reaction		Periosteal reaction		Excessive endosteal reaction		Excessive periosteal reaction	
Group 1 (C)	Left	Right	Left	Right	Left	Right	Left	Right
32	1	1	1	1	2	2	2	2
35	1	1	1	1	2	2	3	2
38	0	1	0	1	2	2	2	2
43	1	1	0	0	2	2	2	2
Group 2 (M)	Left	Right	Left	Right	Left	Right	Left	Right
42	1	1	0	1	2	2	2	2
44	1	1	1	0	2	2	2	2
47	1	1	1	1	3	2	3	3
48	0	1	0	1	2	2	2	2
Group 3 (MAb)	Left	Right	Left	Right	Left	Right	Left	Right
39	1	1	1	1	2	2	2	3
40	1	1	1	1	2	2	2	3
41	1	0	0	0	2	2	2	2
45	0	0	0	0	2	2	2	2
Group 4 (MBMP)	Left	Right	Left	Right	Left	Right	Left	Right
27	1	1	1	1	2	2	2	2
29	1	1	1	1	2	3	2	3
33	1	1	1	1	3	3	3	3
36	1	1	1	1	2	2	3	3
Group 5 (MAbBMP)	Left	Right	Left	Right	Left	Right	Left	Right
18	1	1	1	1	3	3	3	3
30	1	1	1	1	2	2	2	3
34	1	1	1	1	2	2	2	2
37	1	1	1	1	2	2	3	3

Legend: Score 0 = none or minimal reaction; score 1 = moderate or excessive reaction; score 2 = absence of excessive reaction; score 3 = excessive reaction.

Table A.8 Bone Mineral Densities (BMD) and Proportional Change in BMD when Compared to Day 1 for all Goats, Days 1, 14, and 30

Group 1 (C)	BMD (g/cm^2)			Proportional change in BMD	
Goat	Day 1	Day 14	Day 30	D14 - D1	D30 - D1
32	0.434	0.407	0.433	-0.062	-0.002
35	1.030	0.559	0.457	-0.457	-0.556
38	0.326	0.514	0.428	0.577	0.313
43	1.013	1.037	1.095	0.024	0.081
Average	*0.701*	*0.629*	*0.603*	.	.
Group 2 (M)	Day 1	Day 14	Day 30	D14 - D1	D30 - D1
42	0.467	0.721	0.428	0.544	-0.084
44	0.488	0.367	0.496	-0.248	0.016
47	1.041	0.634	1.157	-0.391	0.111
48	0.342	0.330	0.447	-0.035	0.307
Average	*0.585*	*0.513*	*0.632*	.	.
Group 3 (MAb)	Day 1	Day 14	Day 30	D14 - D1	D30 - D1
39	0.840	0.851	0.929	0.013	0.106
40	1.159	1.189	1.233	0.026	0.064
41	0.900	0.905	0.944	0.006	0.049
45	0.355	0.368	0.495	0.037	0.394
Average	*0.814*	*0.828*	*0.900*	.	.
Group 4 (MBMP)	Day 1	Day 14	Day 30	D14 - D1	D30 - D1
27	0.556	0.941	1.015	0.692	0.826
29	0.477	0.345	0.393	-0.277	-0.176
33	0.768	0.453	0.464	-0.410	-0.396
36	0.978	0.544	0.517	-0.444	-0.471
Average	*0.695*	*0.571*	*0.597*	.	.
Group 5 (MAbBMP)	Day 1	Day 14	Day 30	D14 - D1	D30 - D1
18	0.998	1.049	1.153	0.051	0.155
30	0.682	0.499	0.446	-0.268	-0.346
34	1.147	1.203	1.208	0.049	0.053
37	0.898	0.462	0.432	-0.486	-0.519
Average	*0.931*	*0.803*	*0.810*	.	.

Table A.9 Plasma Concentration of Tigecycline for all Goats in Groups 3 & 5, Days 0-30

Time (days)	Group 3 (MAb) Tigecycline concentration (ng/ml)				Group 5 (MAbBMP) Tigecycline concentration (ng/ml)			
	Goat 39	Goat 40	Goat 41	Goat 45	Goat 18	Goat 30	Goat 34	Goat 37
0	0	0	0	0	0	0	0	0
1	4.0	3.1	5.9	3.0	4.3	3.1	3.9	3.4
2	3.2	·	3.1	2.8	3.3	2.8	3.2	3.1
3	2.4	3.8	3.0	2.6	3.2	2.7	3.3	2.9
4	·	3.5	2.7	2.6	3.4	2.6	3.2	3.2
5	·	3.2	2.8	2.5	3.5	2.9	3.5	2.9
6	2.5	3.4	2.7	2.9	·	2.7	3.7	3.6
7	2.9	3.1	·	2.6	3.3	3.2	3.1	3.3
9	3.1	3.9	·	2.5	3.1	2.5	3.4	3.3
11	2.8	3.5	3.3	2.4	2.7	2.4	3.0	2.9
13	3.3	2.8	3.4	2.7	2.5	2.5	2.9	3.1
15	2.7	2.9	3.2	2.6	2.6	2.5	3.3	3.0
17	2.6	3.2	3.8	2.6	0	2.4	2.5	3.6
22	2.1	2.7	2.3	2.4	0	2.3	2.7	0
26	0	2.1	0	2.2	0	2.4	2.6	0
30	·	2.1	0	2.2	0	2.5	0	0

Table A.10 Plasma Concentration of Tobramycin for all Goats in Groups 3 & 5, Days 0-30

Time (days)	Group 3				Group 5			
	Tobramycin concentration (ng/ml)				Tobramycin concentration (ng/ml)			
	Goat 39	Goat 40	Goat 41	Goat 45	Goat 18	Goat 30	Goat 34	Goat 37
0	.	.	0	0	0	0	0	0
1	.	2.5	.	1.4	5.7	3.1	6.1	4.8
2	2.5	2.3	1.6	1.4	3.6	3.0	4.6	3.7
3	2.2	2.4	1.4	.	2.8	2.8	3.5	2.8
4	2.2	.	1.6	.	2.9	2.5	.	2.6
5	3.8	6.3	5.7	1.4	.	2.8	3.0	2.6
6	3.3	4.5	4.1	8.2	.	2.4	2.6	2.1
7	2.6	3.1	2.6	5.6	.	2.4	2.7	.
9	.	2.8	.	3.0	2.6	2.4	2.8	2.5
11	2.5	2.2	2.0	2.5	2.4	2.5	2.4	.
13	.	2.4	1.8	2.2	2.5	2.7	3.0	.
15	2.5	1.7	1.8	1.6	2.6	2.3	2.6	.
17	2.2	1.7	1.5	1.7	2.5	2.7	2.6	2.6
22	.	1.9	1.6	1.5	2.5	.	.	2.5
26	.	.	1.3	.	.	.	.	2.3
30	.	1.9	1.4	1.5	2.7	.	.	.

Table A.11 Mean ± SEM Plasma Concentrations of Tigecycline & Tobramycin for all Goats in Groups 3 & 5, Days 0-30

| Time (days) | Tigecycline concentration (ng/ml) | | Tobramycin concentration (ng/ml) | | | |
| | Groups 3 and 5 | | Group 3 | | Group 5 | |
	Least Square Mean	Standard Error	Least Square Mean	Standard Error	Least Square Mean	Standard Error
0	0.0	0.3	0.0	0.6	0.0	0.4
1	3.8	0.3	2.0	0.6	4.9	0.4
2	3.1	0.3	2.0	0.4	3.7	0.4
3	3.0	0.3	2.0	0.5	3.0	0.4
4	3.0	0.3	1.9	0.6	2.7	0.5
5	3.0	0.3	4.3	0.4	2.8	0.5
6	3.0	0.3	5.0	0.4	2.4	0.5
7	3.1	0.3	3.5	0.4	2.5	0.6
9	3.1	0.3	2.9	0.6	2.6	0.4
11	2.9	0.3	2.3	0.4	2.4	0.5
13	2.9	0.	2.2	0.5	2.7	0.5
15	2.9	0.3	1.9	0.4	2.5	0.5
17	2.6	0.3	1.7	0.4	2.6	0.4
22	1.8	0.3	1.7	0.5	2.5	0.6
26	1.1	0.3	1.3	0.9	2.3	0.9
30	1.0	0.3	1.6	0.5	2.7	0.9

Table A.12 LS Means Differences Student's t for Plasma Concentration of Tigecycline

Level (day)					Least Square Mean
1	A				3.833
9	A	B			3.119
2		B			3.082
7		B			3.063
5		B			3.036
6		B			3.029
4		B			3.010
3		B			2.993
13		B			2.908
11		B			2.876
15		B			2.851
17		B			2.580
22			C		1.809
26			C	D	1.143
30				D	0.974
0					E	0.000

Levels not connected by same letter are significantly different (α = 0.05).

Table A.13 LS Means Differences Student's t for Plasma Concentration of Tobramycin

Level (Tx,day)								Least Square Mean
3,6	A							5.025
5,1	A							4.930
3,5	A	B						4.290
5,2		B	C					3.710
3,7		B	C	D				3.470
5,3			C	D	E			2.955
3,9		B	C	D	E	F		2.907
5,5			C	D	E	F		2.789
5,13			C	D	E	F		2.742
5,4			C	D	E	F		2.669
5,30		B	C	D	E	F		2.663
5,17			C	D	E	F		2.600
5,9			C	D	E	F		2.583
5,7			C	D	E	F		2.516
5,22			C	D	E	F		2.489
5,15			C	D	E	F		2.472
5,11			C	D	E	F		2.445
5,6				D	E	F		2.352
3,11				D	E	F		2.305
5,26			C	D	E	F		2.295
3,13					E	F		2.165
3,3					E	F		1.984
3,1					E	F		1.967
3,2					E	F		1.940
3,15					E	F		1.918
3,4					E	F		1.888
3,17						F		1.745
3,22						F		1.658
3,30						F		1.602
3,26					E	F	G	1.321
5,0							G	0.000
3,0							G	0.000

Levels not connected by same letter are significantly different ($\alpha = 0.05$).

Table A.14 Serum Concentration of rhBMP-2 for all Goats from all Groups, Days 0-30

	Serum concentration of rhBMP-2 (pg/ml)							
	Group 1 (C)				Group 2 (M)			
Time (days)	Goat 32	Goat 35	Goat 38	Goat 43	Goat 42	Goat 44	Goat 47	Goat 48
0	87.0	73.7	73.7	78.7	87.0	73.7	70.3	67.0
1	72.0	57.0	73.7	73.7	78.7	70.3	72.0	68.7
2	83.7	68.7	20.3	18.7	20.3	12.0	18.7	25.3
3	35.3	18.7	17.0	.	18.7	13.7	13.7	15.3
4	27.0	13.7	96.0	89.3	89.3	89.3	89.3	101.0
5	104.3	96.0	87.7	96.0	96.0	82.7	84.3	82.7
6	99.3	86.0	103.7	88.7	88.7	95.3	97.0	103.7
7	100.3	97.0	147.0	100.3	92.0	82.0	85.3	88.7
9	47.8	32.8	34.0	40.3	37.8	35.3	34.0	34.0
11	44.0	29.0	34.0	36.5	36.5	37.8	36.5	40.3
13	39.0	32.8	31.5	32.8	30.3	166.5	22.8	26.5
15	39.0	24.0	29.0	30.3	31.5	29.0	31.5	35.3
17	52.3	39.8	39.8	39.8	38.5	37.3	33.5	41.0
22	104.8	48.5	44.8	44.8	42.3	43.5	48.5	43.5
25	48.7	30.3	38.7	37.0	37.0	33.7	27.0	37.0
30	55.3	33.7	38.7	48.7	43.7	45.3	43.7	48.7
	Group 3 (MAb)				Group 4 (MBMP)			
Time (days)	Goat 39	Goat 40	Goat 41	Goat 45	Goat 27	Goat 29	Goat 33	Goat 36
0	77.0	82.0	78.7	73.7	75.3	67.0	90.3	77.0
1	72.0	75.3	75.3	68.7	97.0	63.7	67.0	67.0
2	25.3	13.7	25.3	20.3	82.0	80.3	83.7	75.3
3	10.3	15.3	18.7	18.7	27.0	15.3	38.7	12.0
4	99.3	89.3	112.7	107.7	107.0	17.0	42.0	17.0
5	86.0	89.3	96.0	92.7	111.0	89.3	109.3	89.3
6	100.3	90.3	102.0	93.7	97.7	89.3	104.3	89.3
7	85.3	87.0	88.7	93.7	98.7	85.3	103.7	87.0
9	35.3	35.3	40.3	36.5	39.0	34.0	47.8	34.0
11	36.5	39.0	37.8	41.5	40.3	34.0	42.8	34.0
13	24.0	27.8	39.0	31.5	40.3	30.3	39.0	74.0
15	31.5	35.3	34.0	32.8	31.5	30.3	35.3	26.5
17	39.8	36.0	39.8	42.3	56.0	37.3	49.8	39.8
22	46.0	167.3	184.8	46.0	43.5	43.5	51.0	39.8
25	38.7	37.0	40.3	43.7	45.3	37.0	52.0	35.3
30	32.0	50.3	45.3	52.0	38.7	35.3	52.0	32.0

con't	Serum concentration of rhBMP-2 (pg/ml)			
	Group 5 (MAbBMP)			
Time (days)	Goat 18	goat 30	Goat 34	Goat 37
0	78.7	88.7	75.3	77.0
1	53.7	53.7	60.3	68.7
2	72.0	67.0	72.0	83.7
3	13.7	18.7	22.0	18.7
4	12.0	17.0	17.0	25.3
5	87.7	84.3	92.7	96.0
6	94.3	94.3	87.7	99.3
7	85.3	85.3	95.3	97.0
9	36.5	32.8	35.3	36.5
11	32.8	35.3	32.8	37.8
13	54.0	27.8	29.0	36.5
15	26.5	29.0	26.5	30.3
17	39.8	43.5	44.8	46.0
22	34.8	37.3	39.8	42.3
25	32.0	40.3	45.3	53.7
30	33.7	30.3	32.0	42.0

Table A.15 Mean ± SEM Serum Concentration of rhBMP-2 of all Goats from all Groups, Days 0-30

	Serum concentration of rhBMP-2 (pg/ml)									
	Group 1 (C)		Group 2 (M)		Group 3 (MAb)		Group 4 (MBMP)		Group 5 (MAbBMP)	
Time (days)	Least Square Mean	Standard Error	Least Square Mean	Standard Error	Least Square Mean	Standard Error	Least Square Mean	Standard Error	Least Square Mean	Standard Error
0	78.3	7.9	74.5	7.9	77.8	7.9	77.4	7.9	79.9	7.9
1	69.1	7.9	72.4	7.9	72.8	7.9	73.7	7.9	59.1	7.9
2	47.8	7.9	19.1	7.9	21.2	7.9	80.3	7.9	73.7	7.9
3	23.4	9.1	15.3	7.9	15.8	7.9	23.3	7.9	18.3	7.9
4	56.5	7.9	92.3	7.9	102.3	7.9	45.8	7.9	17.8	7.9
5	96.0	7.9	86.4	7.9	91.0	7.9	99.8	7.9	90.2	7.9
6	94.4	7.9	96.2	7.9	96.6	7.9	95.2	7.9	93.9	7.9
7	111.2	7.9	87.0	7.9	88.7	7.9	93.7	7.9	90.8	7.9
9	38.7	7.9	35.3	7.9	36.8	7.9	38.7	7.9	35.3	7.9
11	35.9	7.9	37.8	7.9	38.7	7.9	37.8	7.9	34.6	7.9
13	34.0	7.9	61.5	7.9	30.6	7.9	45.9	7.9	36.8	7.9
15	30.6	7.9	31.8	7.9	33.4	7.9	30.9	7.9	28.1	7.9
17	42.9	7.9	37.6	7.9	39.4	7.9	45.7	7.9	43.5	7.9
22	60.7	7.9	44.4	7.9	111.0	7.9	44.4	7.9	38.5	7.9
25	38.7	7.9	33.7	7.9	39.9	7.9	42.4	7.9	42.8	7.9
30	44.1	7.9	45.3	7.9	44.9	7.9	39.5	7.9	34.5	7.9

Table A.16 LS Means Differences Student's t for Mean Serum Concentration of rhBMP-2

Level (Tx, days)	A	B	C	D	E	F	G	H	I	J	K	L	M	N	O	P	Q	Least Squares Mean
1,7	A																	111.167
3,22	A																	111.000
3,4	A	B																102.250
4,5	A	B	C															99.750
3,6	A	B	C	D	E													96.583
2,6	A	B	C	D														96.167
1,5	A	B	C	D	E													96.000
4,6	A	B	C	D	E	F												95.167
1,6	A	B	C	D	E	F	G											94.417
5,6	A	B	C	D	E	F	G											93.917
4,7	A	B	C	D	E	F	G											93.667
2,4	A	B	C	D	E	F	G											92.250
3,5	A	B	C	D	E	F	G	H										91.000
5,7	A	B	C	D	E	F	G	H										90.750
5,5	A	B	C	D	E	F	G	H										90.167
3,7		B	C	D	E	F	G	H										88.667
2,7		B	C	D	E	F	G	H										87.000
2,5		B	C	D	E	F	G	H										86.417
4,2		B	C	D	E	F	G	H	I									80.333
5,0			C	D	E	F	G	H	I									79.917
1,0			C	D	E	F	G	H	I									78.250
3,0			C	D	E	F	G	H	I	J								77.833
4,0				D	E	F	G	H	I	J								77.417
2,0					E	F	G	H	I	J								74.500
4,1							G	H	I	J								73.667
5,2						F	G	H	I	J								73.667
3,1							G	H	I	J								72.833
2,1							G	H	I	J								72.417
1,1								H	I	J	K							69.083
2,13									I	J	K	L						61.500
1,22									I	J	K	L	M					60.688
5,1									I	J	K	L	M	N				59.083
1,4										J	K	L	M	N	O			56.500
1,2											K	L	M	N	O	P		47.833
4,13												L	M	N	O	P	Q	45.875
4,4												L	M	N	O	P	Q	45.750

	L	M	N	O	P	Q	R	S	T	U	V	
4,17	L	M	N	O	P	Q						45.688
2,30	L	M	N	O	P	Q	R					45.333
3,30	L	M	N	O	P	Q	R					44.917
2,22	L	M	N	O	P	Q	R					44.438
4,22	L	M	N	O	P	Q	R					44.438
1,30	L	M	N	O	P	Q	R					44.083
5,17	L	M	N	O	P	Q	R					43.500
1,17	L	M	N	O	P	Q	R	S				42.875
5,25	L	M	N	O	P	Q	R	S				42.833
4,25	L	M	N	O	P	Q	R	S				42.417
3,25	L	M	N	O	P	Q	R	S	T			39.917
4,30	L	M	N	O	P	Q	R	S	T			39.500
3,17	L	M	N	O	P	Q	R	S	T			39.438
4,9		M	N	O	P	Q	R	S	T			38.688
1,9			N	O	P	Q	R	S	T			38.688
3,11		M	N	O	P	Q	R	S	T			38.688
1,25			N	O	P	Q	R	S	T			38.667
5,22			N	O	P	Q	R	S	T			38.500
2,11			N	O	P	Q	R	S	T	U		37.750
4,11			N	O	P	Q	R	S	T	U		37.750
2,17			N	O	P	Q	R	S	T	U		37.563
5,13				O	P	Q	R	S	T	U	V	36.813
3,9				O	P	Q	R	S	T	U	V	36.813
1,11				O	P	Q	R	S	T	U	V	35.875
2,9				O	P	Q	R	S	T	U	V	35.250
5,9				O	P	Q	R	S	T	U	V	35.250
5,11				O	P	Q	R	S	T	U	V	34.625
5,30				O	P	Q	R	S	T	U	V	34.500
1,13					P	Q	R	S	T	U	V	34.000
2,25					P	Q	R	S	T	U	V	33.667
3,15					P	Q	R	S	T	U	V	33.375
2,15					P	Q	R	S	T	U	V	31.813
4,15					P	Q	R	S	T	U	V	30.875
1,15					P	Q	R	S	T	U	V	30.563
3,13					P	Q	R	S	T	U	V	30.563
5,15					P	Q	R	S	T	U	V	28.063
1,3						Q	R	S	T	U	V	23.390
4,3							R	S	T	U	V	23.250
3,2								S	T	U	V	21.167
2,2									T	U	V	19.083
5,3									T	U	V	18.250

5,4				T	U	V	17.833
3,3					U	V	15.750
2,3						V	15.333

Levels not connected by same letter are significantly different (α = 0.05).

Table A.17 Subjective Gross Evaluation of Periosteal & Endosteal Reactions on Histological Slides Using a Binomial Scoring System, Day 30

Groups	Goat (hind limb)	Periosteal reaction	Endosteal reaction
1 (C)	32 (right)	2	1
	35 (right)	2	1
	38 (left)	2	1
	43 (right)	2	1
2 (M)	42 (right)	2	2
	44 (left)	2	1
	47 (right)	2	2
	48 (left)	1	1
3 (MAb)	39 (left)	2	2
	40 (left)	1	2
	41 (left)	1	2
	45 (right)	1	2
4 (MBMP)	27 (left)	2	2
	29 (left)	2	2
	33 (right)	2	2
	36 (right)	2	1
5 (MAbBMP)	18 (left)	2	2
	30 (left)	2	2
	34 (right)	2	2
	37 (left)	2	2

Legend: score 1 = none or minimal reaction; score 2 = moderate to severe reaction.

Table A.18 Probability That a Goat From a Given Group had No or Minimal Endosteal Reaction Upon Gross Evaluation of the Histological Slides, Day 30

Groups	Probability
1 (C)	1.00
2 (M)	0.50
3 (MAb)	0
4 (MBMP)	0.25
5 (MAbBMP)	0

Table A.19 Qualitative Gross Evaluation of Surface of Periosteal & Endosteal Reactions and Surface of Endosteal Reaction:Surface of Medullary Cavity Ratio on Histological Slides Using a Digital Caliper, Day 30

		Periosteal reaction			Endosteal reaction			Medullary cavity			Proportion
Gr	Goat (hindlimb)	Width (mm)	Length (mm)	Area (mm^2)	Width (mm)	Length (mm)	Area (mm^2)	Width (mm)	Length (mm)	Area (mm^2)	Endos. Rx / medul. cavit.
1 (C)	32 (right)	2.81	11.86	33.33	0.48	1.09	0.52	12.71	13.31	169.17	0.0031
	35 (right)	1.37	21.69	29.72	0.7	0.74	0.52	14.21	12.64	179.61	0.0029
	38 (left)	1.2	22.54	27.05	1.44	0.65	0.94	14.74	12.55	184.99	0.0051
	43 (right)	1.76	14.67	25.82	0.47	3.41	1.60	9.46	9.44	89.30	0.0179
2 (M)	42 (right)	1.98	11.28	22.33	7.06	8.18	57.75	9.68	8.18	79.18	0.7293
	44 (left)	1.44	16.76	24.13	6.4	8.07	51.65	11.77	13.54	159.37	0.3241
	47 (right)	2.54	15.58	39.57	6.26	8.16	51.08	10.67	9.59	102.33	0.4992
	48 (left)	0.86	23.91	20.56	4.8	9.94	47.71	17.61	16.66	293.38	0.1626
3 (MAb)	39 (left)	2.53	17.49	44.25	6.84	10.56	72.23	11.97	11.27	134.90	0.5354
	40 (left)	0.98	14.34	14.05	5.29	8.72	46.13	8.83	8.72	77.00	0.5991
	41 (left)	0.39	12.87	5.02	6.84	7.6	51.98	10.25	9.57	98.09	0.5299
	45 (right)	0.28	15.61	4.37	6.85	10.5	71.93	11.73	12.12	142.17	0.5059
4 (MBMP)	27 (left)	4.57	19.77	90.35	9.75	9.11	88.82	10.1	10.09	101.91	0.8716
	29 (left)	1.73	15.11	26.14	9.07	13.08	118.64	13.07	13.08	170.96	0.6940
	33 (right)	4.28	21.47	91.89	8.94	11.68	104.42	12.82	12.5	160.25	0.6516
	36 (right)	4.04	18.48	74.66	8.1	8.56	69.34	14.33	13.28	190.30	0.3643
5 (MAbBMP)	18 (left)	4.77	17.6	83.95	5.38	8.67	46.64	10.24	9.84	100.76	0.4629
	30 (left)	1.58	12.18	19.24	5.2	9.6	49.92	11.18	11.99	134.05	0.3724
	34 (right)	2.18	6.76	14.74	6.36	8.7	55.33	12.53	12.57	157.50	0.3513
	37 (left)	2.59	18.74	48.54	6.62	6.74	44.62	10.69	10.4	111.18	0.4013

Table A.20 Mean ± SEM Surface of Periosteal & Endosteal Reactions and Mean ± SEM Surface of Endosteal Reaction:Surface of Medullary Cavity Ratio as Qualitatively Evaluated Using a Digital Caliper, Day 30

Group	Periosteal rx area (mm^2)		Endosteal reaction area (mm^2)		Proport. endosteal rx / medull. cav.	
	Least Square Mean	Standard Error	Least Square Mean	Standard Error	Least Square Mean	Standard Error
1 (C)	28.98	10.97	0.89	5.79	0.0072	0.0732
2 (M)	26.65	10.97	52.05	5.79	0.4288	0.0732
3 (MAb)	16.92	10.97	60.57	5.79	0.5426	0.0732
4 (MBMP)	70.76	10.97	95.30	5.79	0.6454	0.0732
5 (MAbBMP)	41.62	10.97	49.13	5.79	0.3970	0.0732

Table A.21 LS Means Differences Student's t for Mean Surface of Periosteal Reaction Determined by Qualitative Gross Evaluation (Digital Caliper) of the Histological Slides

Surface of periosteal reaction (mm^2)			
Level (group)			Least Squares Mean
4	A		70.76
5	A	B	41.62
1		B	28.98
2		B	26.65
3		B	16.92

Levels not connected by same letter are significantly different (α = 0.05).

Table A.22 LS Means Differences Student's t for Mean Surface of Endosteal Reaction Determined by Qualitative Gross Evaluation (Digital Caliper) of the Histological Slides

Surface of endosteal reaction (mm^2)			
Level (group)			Least Squares Mean
4	A		95.30
3		B	60.57
2		B	52.05
5		B	49.13
1		C	0.89

Levels not connected by same letter are significantly different (α = 0.05).

Table A.23 Percent Filling of Bone Defect Evaluated Using Red Channels Images for all Goats from all Groups, Day 30

Group	Goat (hind limb)	Rolling ball radius (pixels)	Resolution (pixels/um)	Area of interest (µm^2)	% bone filling
1 (C)	32 (right)	50	0.180	4509787.74	36.46
	35 (right)	50	0.200	2037196.63	32.47
	38 (left)	50	0.200	1931065.21	32.02
	43 (right)	50	0.204	4675358.09	43.03
2 (M)	42 (right)	50	0.215	7101342.75	58.07
	44 (left)	50	0.180	4149434.45	42.81
	47 (right)	50	0.201	5387399.06	45.15
	48 (left)	50	0.206	2182960.90	39.74
3 (MAb)	39 (left)	50	0.194	2337628.31	29.32
	40 (left)	50	0.193	5274062.89	43.30
	41 (left)	50	0.158	4139646.13	31.59
	45 (right)	50	0.210	3155045.84	33.36
4 (MBMP)	27 (left)	50	0.167	3047995.78	23.69
	29 (left)	50	0.178	3456462.72	49.54
	33 (right)	50	0.138	2566649.71	26.55
	36 (right)	50	0.203	3090864.21	31.74
5 (MAbBMP)	18 (left)	50	0.150	5542739.82	36.30
	30 (left)	200	0.200	6434956.31	50.59
	34 (right)	100	0.218	1951966.00	17.24
	37 (left)	50	0.154	3872465.66	32.56

Threshold was set at 149 for all red channels image analysis.

Table A.24 Percent Filling of Bone Defect Evaluated Using Green Channels Images for all Goats from all Groups, Day 30

Group	Goat (hind limb)	Area (μm^2)	% bone filling
1 (C)	32 (right)	4494916.93	36.34
	35 (right)	1731579.60	27.60
	38 (left)	1864363.94	30.92
	43 (right)	4496312.61	41.38
2 (M)	42 (right)	6953885.49	56.86
	44 (left)	4124225.06	42.55
	47 (right)	5434039.67	45.54
	48 (left)	2121027.09	38.61
3 (MAb)	39 (left)	2349240.23	29.47
	40 (left)	4222214.70	34.66
	41 (left)	4165566.45	31.79
	45 (right)	3104144.51	32.82
4 (MBMP)	27 (left)	2585431.09	20.09
	29 (left)	3051746.09	43.74
	33 (right)	2478200.99	25.64
	36 (right)	2956164.03	30.35
5 (MAbBMP)	18 (left)	5957149.04	39.01
	30 (left)	6284750.85	49.41
	34 (right)	1871911.80	16.53
	37 (left)	3228000.20	27.14

Threshold was set at 149 for all green channels image analysis. Rolling ball radius and resolution were the same for the green channels images as the red channels images.

Table A.25 Percent Filling of Bone Defect Evaluated Using Blue Channels Images for all Goats from all Groups, Day 30

Group	Goat (hind limb)	Area (μm^2)	% Filling	Standard Error
1 (C)	32 (right)	3590470.67	29.03	4.57
	35 (right)	970227.10	15.46	4.57
	38 (left)	1746619.11	28.96	4.57
	43 (right)	3277386.55	30.16	4.57
2 (M)	42 (right)	6810298.45	55.69	4.57
	44 (left)	4014779.43	41.42	4.57
	47 (right)	5549686.55	46.51	4.57
	48 (left)	1847138.87	33.63	4.57
3 (MAb)	39 (left)	2571139.28	32.25	4.57
	40 (left)	3586397.01	29.44	4.57
	41 (left)	4625721.79	35.30	4.57
	45 (right)	3136571.21	33.16	4.57
4 (MBMP)	27 (left)	1587334.77	12.34	4.57
	29 (left)	1021944.38	14.65	4.57
	33 (right)	2380722.59	24.63	4.57
	36 (right)	2274261.03	23.35	4.57
5 (MAbBMP)	18 (left)	6409484.98	41.98	4.57
	30 (left)	6424950.93	50.51	4.57
	34 (right)	2426496.24	21.43	4.57
	37 (left)	2256920.34	18.98	4.57

Threshold was 200 for all blue channels image analysis. Rolling ball radius and resolution were the same for the blue channels images as the red channels images.

Table A.26 Mean ± SEM Percent Filling of Bone Defect Evaluated by Computerized Image Analysis for all Goats from all Groups, Day 30

	Red channels images		Green channels images		Blue channels images	
Group	LS Mean	Standard Error	LS Mean	Standard Error	LS Mean	Standard Error
1 (C)	35.99	4.75	34.06	4.52	25.90	4.57
2 (M)	46.44	4.75	45.89	4.52	44.31	4.57
3 (MAb)	34.39	4.75	32.19	4.52	32.54	4.57
4 (MBMP)	32.88	4.75	29.96	4.52	18.74	4.57
5 (MAbBMP)	34.17	4.75	33.02	4.52	33.22	4.57

Table A.27 LS Means Differences Student's t for Percent Filling of Bone Defect Evaluated by Computerized Image Analysis (Blue Channels Images) for all Goats from all Groups, Day 30

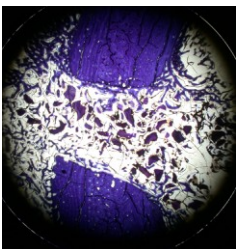| Level (treatment)				Least Squares Mean
2	A			44.31
5	A	B		33.22
3	A	B		32.54
1		B	C	25.90
4			C	18.74

Levels not connected by same letter are significantly different (α = 0.05).

Table A.28 Characteristics of the *in vitro* elution of tobramycin from different non biodegradable and biodegradable local delivery systems for bone

Local delivery system	Duration of release	Mean peak release	Time when peak observed	References
PMMA beads	84 days	34.3 μg/ml	Day 1	[142]
PMMA beads	30 days	234-299 mg/l	Day 1	[146]
PMMA beads	220 days	> 250 mg/l	Day 1	[147]
PLA beads	42 days	N/A	Day 1	
PLGA beads	36-65 days*	N/A	Day 1 & day 25	
PLGA-PEG copolymer	27 days	N/A	Day 1	[49]
Bone graft	7 days	17047 μg/g pellet	Day 1	
Demineralized bone matrix	4 days	11 437 μg/g pellet	Day 1	[50]
Plaster of Paris	4 days	4294 μg/g pellet	Day 1	

Legend: PLGA = poly(DL-lactic-co-glycolic acid); PEG = poly(ethylene glycol); PLA = polylactic acid;* depending on the ratio of DL-lactide and coglycolide; N/A: unavailable information.

Appendix B - Supplementary Figures
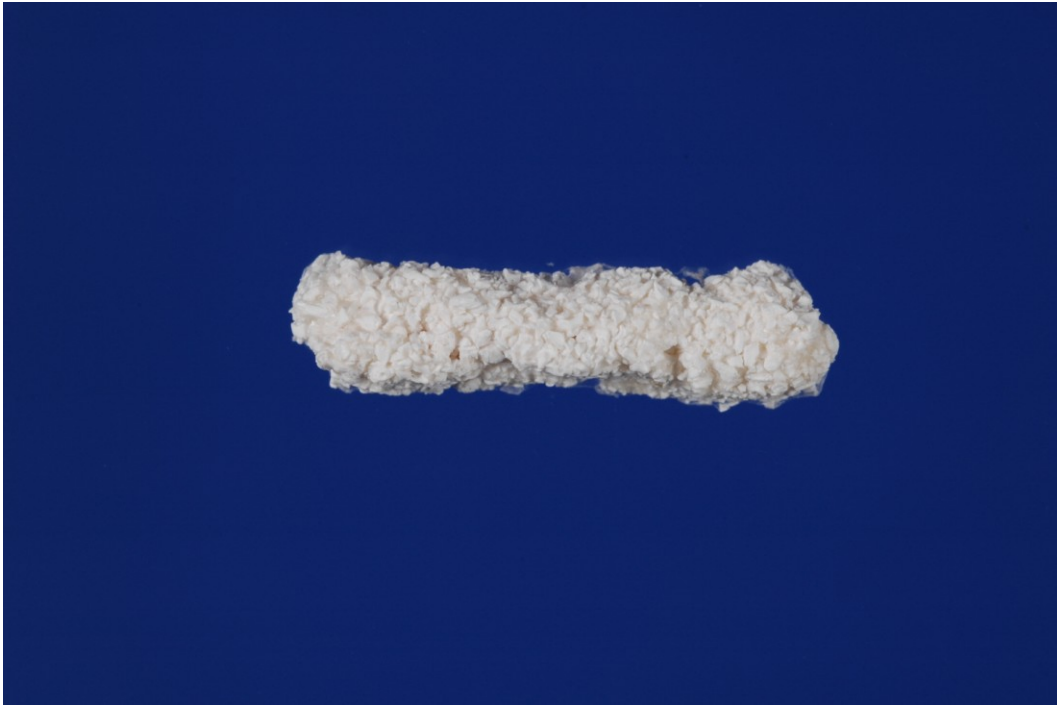
Figure B.1 Photograph of the Novel Polymeric Bone Matrix
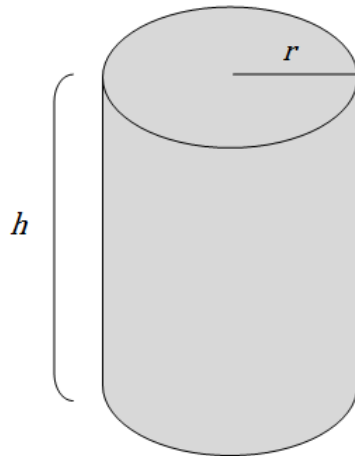
$$v = \pi r^2 h$$

where v is the volume of the cylinder, r is the radius of the circular end of the cylinder, h is the height of the cylinder, and π is Pi, approximately 3.142.

Figure B.2 Equation to compute the volume of a cylinder

$$Proportional\ change\ in\ BMD = \frac{BMD_n - BMD_0}{BMD_0}$$

where BMD_n is the bone mineral density on day n, and BMD_0 is the initial bone mineral density (measured on day 1).

Figure B.3 Equation used to compute the percent change in BMD on day 14 and 30
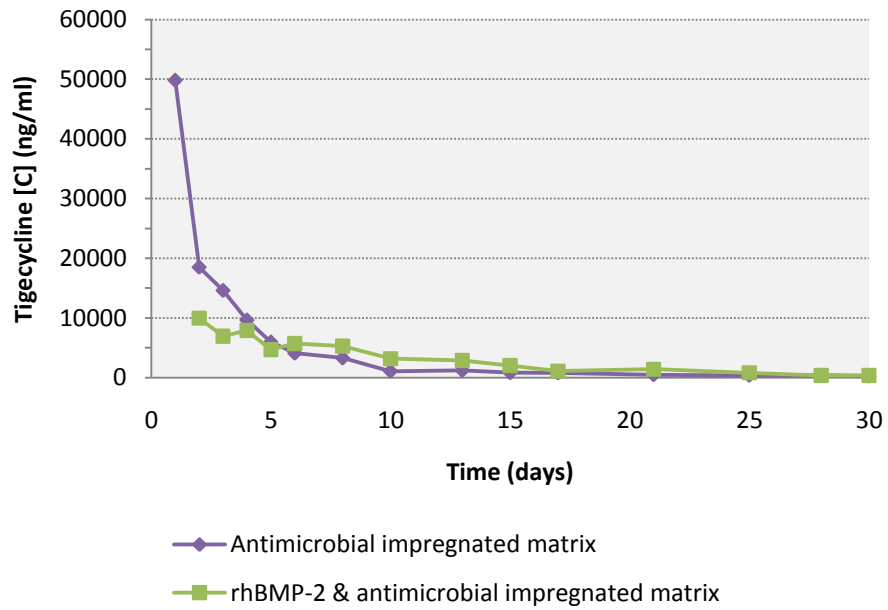
Figure B.4 *In Vitro* Elution Curve of Tigecycline from the Novel Polymeric Bone Matrix
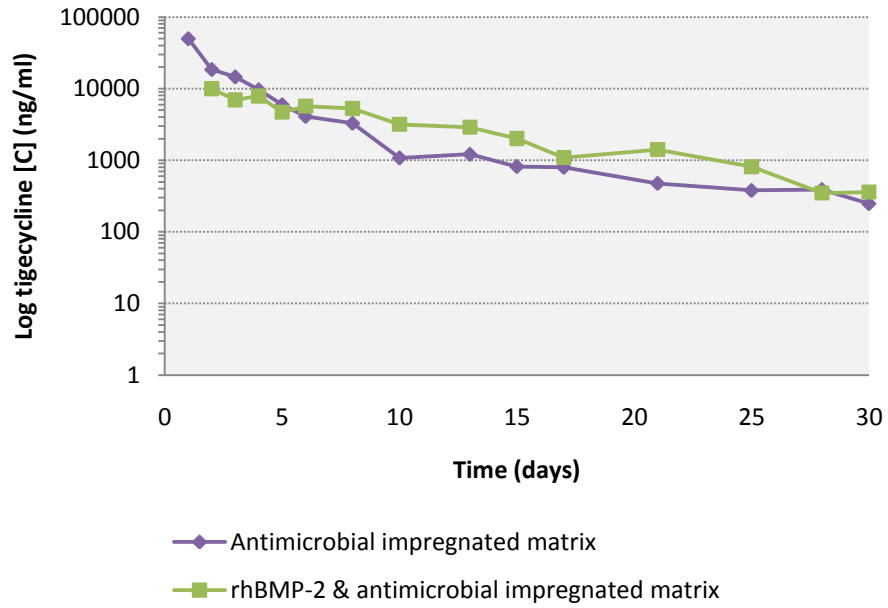
Figure B.5 *In Vitro* Elution Curve of Tigecycline from the Matrix Using a log$_{10}$ Vertical Axis
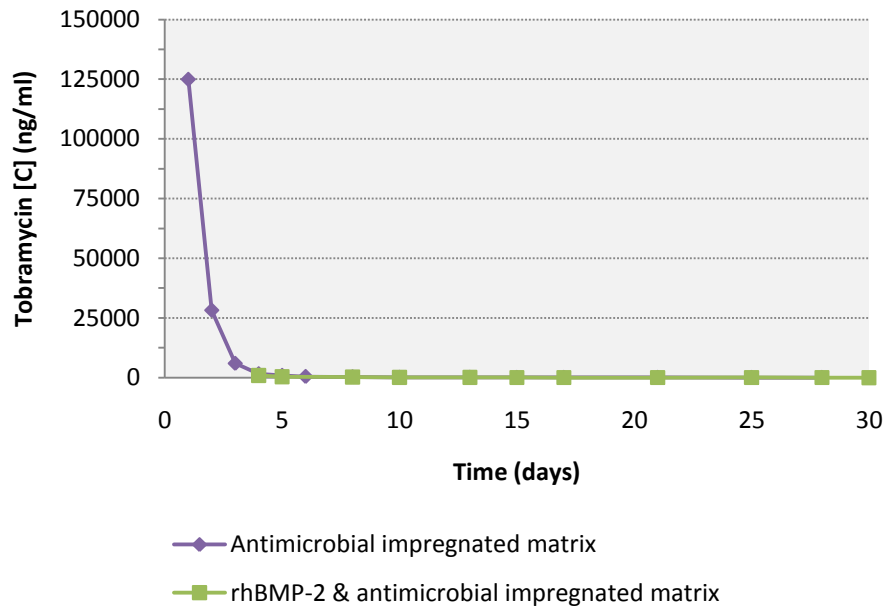
Figure B.6 *In Vitro* **Elution Curve of Tobramycin From the Matrix**
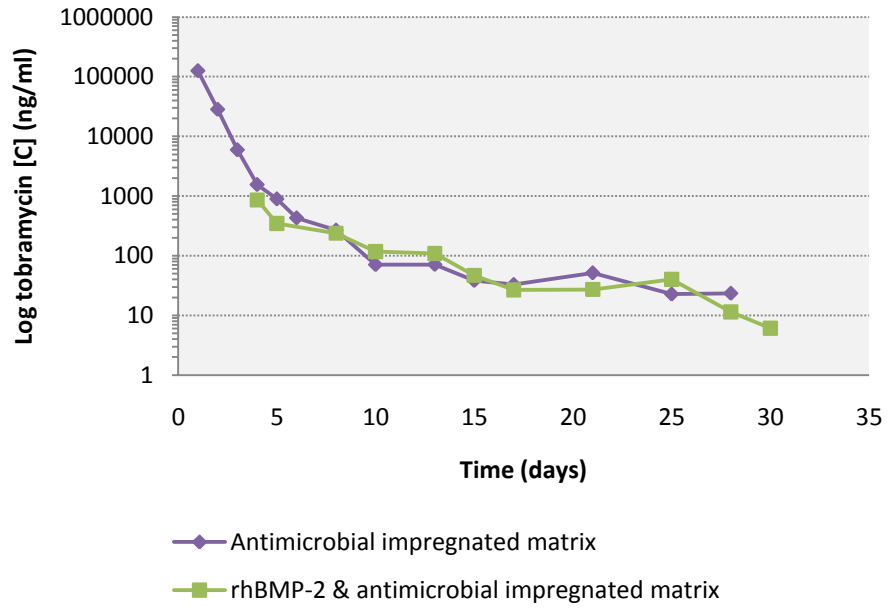
Figure B.7 *In Vitro* **Elution Curve of Tobramycin from the Matrix Using a $\log_{10}$ Vertical Axis**
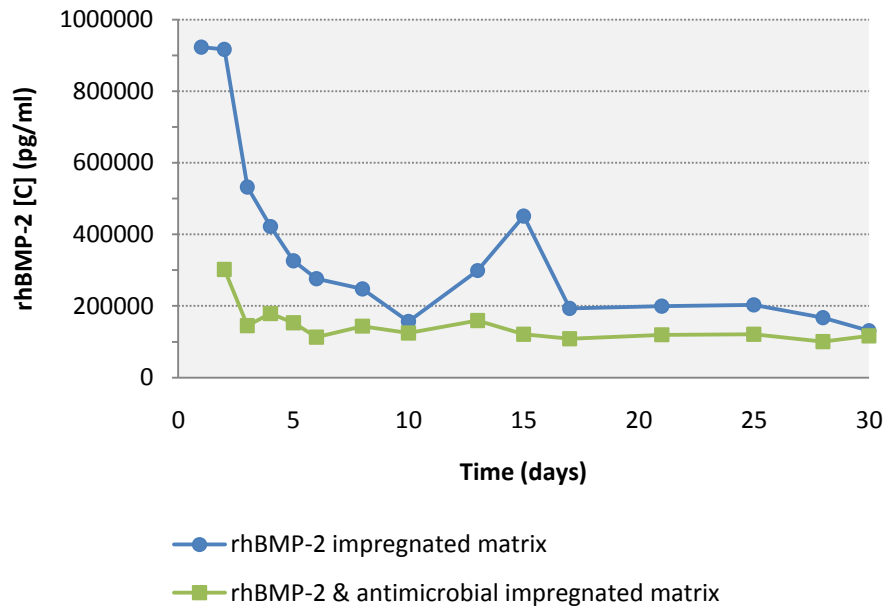
Figure B.8 *In Vitro* **Elution Curve of rhBMP-2 From the Matrix**
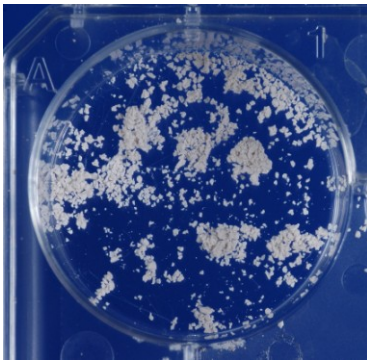
Figure B.9 Integrity of the Antimicrobial Impregnated Matrix at the End of the *In Vitro* Experiment, Day 30
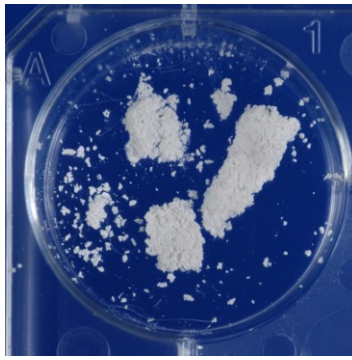
Figure B.10 Integrity of the rhBMP-2 Impregnated Matrix at the End of the *In Vitro* Experiment, Day 30
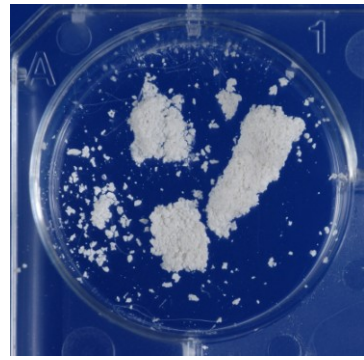
Figure B.11 Integrity of the Co-impregnated Matrix at the End of the *In Vitro* Experiment, Day 30
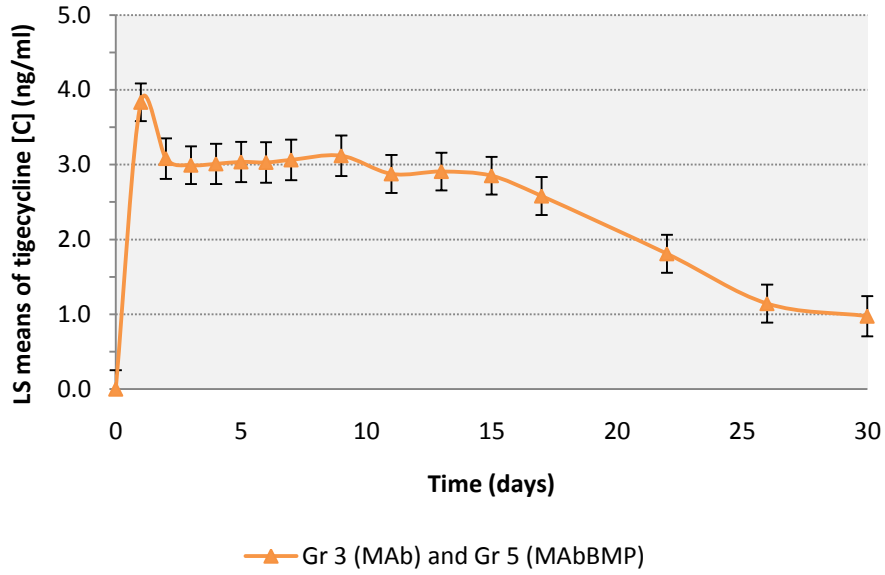
Figure B.12 Mean ± SEM Plasma Concentration of Tigecycline in Groups 3 & 5, Days 0-30
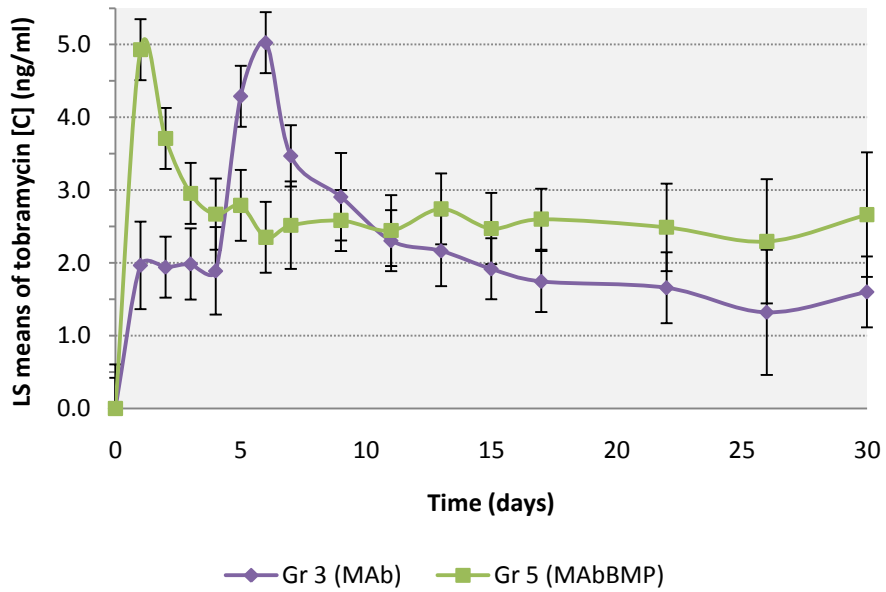
Figure B.13 Mean ± SEM Plasma Concentration of Tobramycin in Groups 3 & 5, Days 0-30
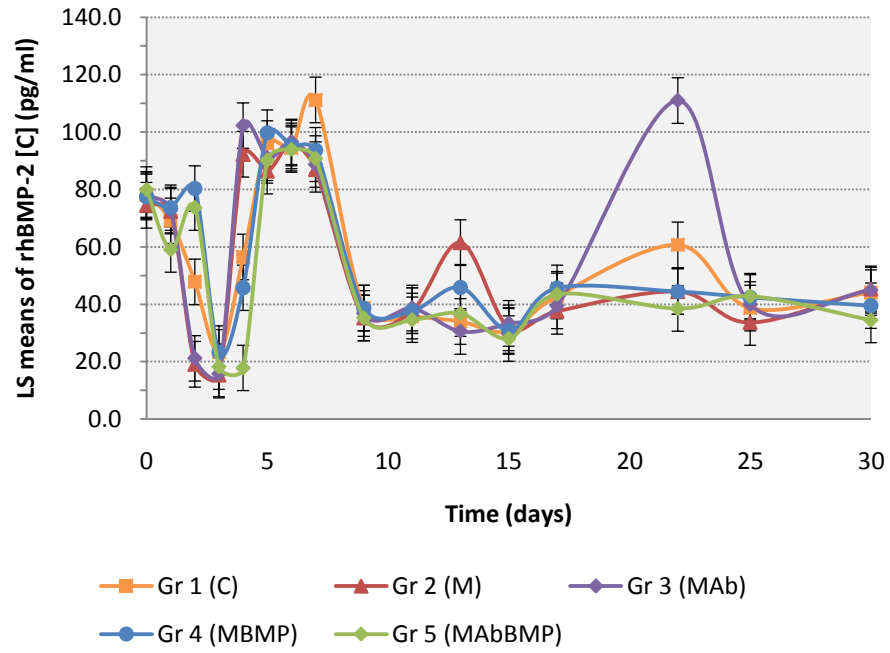
Figure B.14 Mean ± SEM Serum Concentration of rhBMP-2 for all Groups, Days 0-30
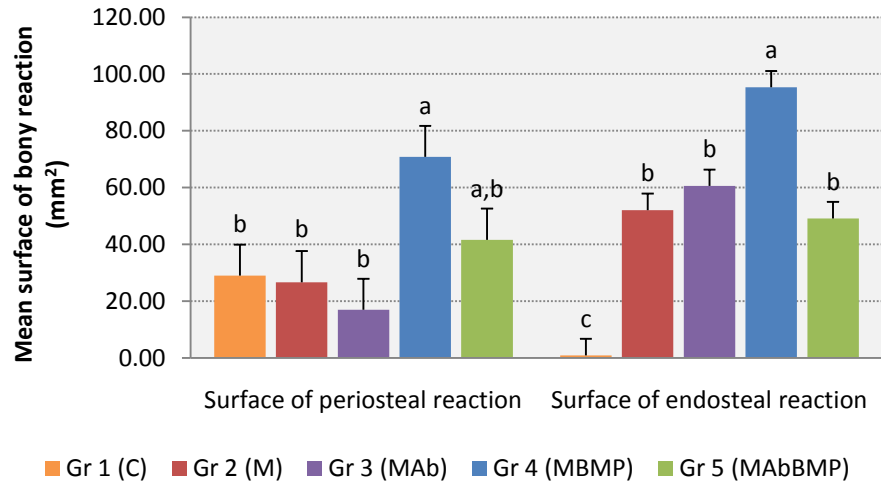
Figure B.15 Effect of Treatment on Mean Surface of Periosteal and Endosteal Reaction for all Groups, Day 30
Bars that share a letter (a-c) are not statistically different at P < 0.05.
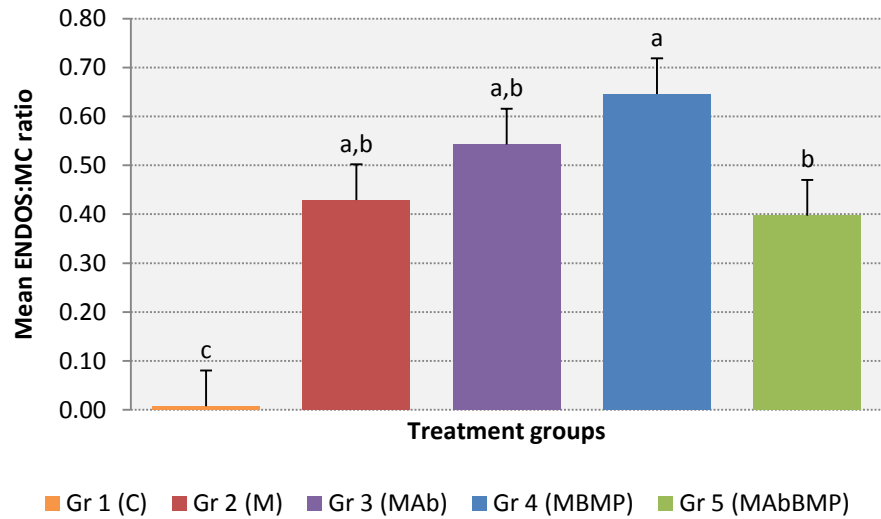
Figure B.16 Effect of Treatment on Surface of Endosteal Reaction:Medullary Cavity Ratio for all Groups, Day 30
Bars that share a letter (a-b) are not statistically different at $P < 0.05$.
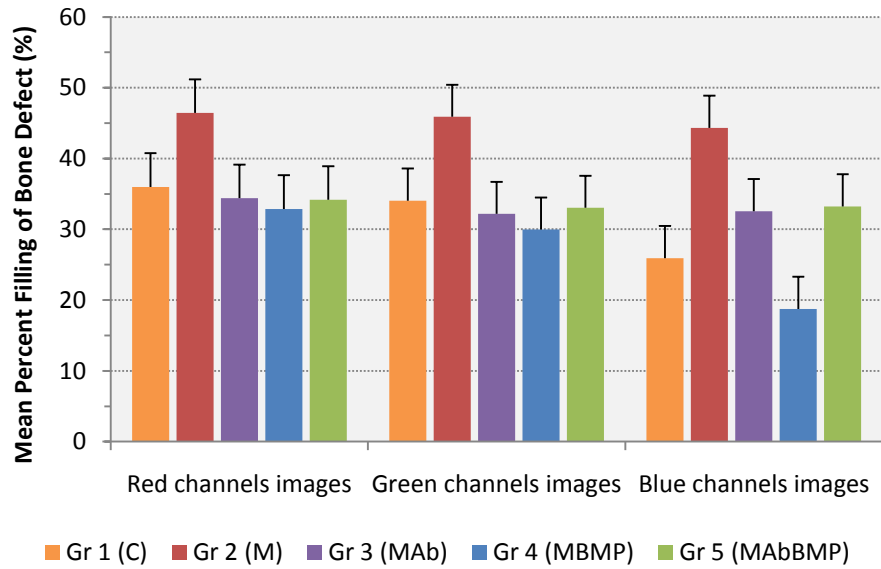
Figure B.17 Mean Percent Filling of Bone Defects Evaluated by Computerized Image Analysis of the Three Fragmented Images (Red, Green, and Blue Channels) for all Groups, Day 30
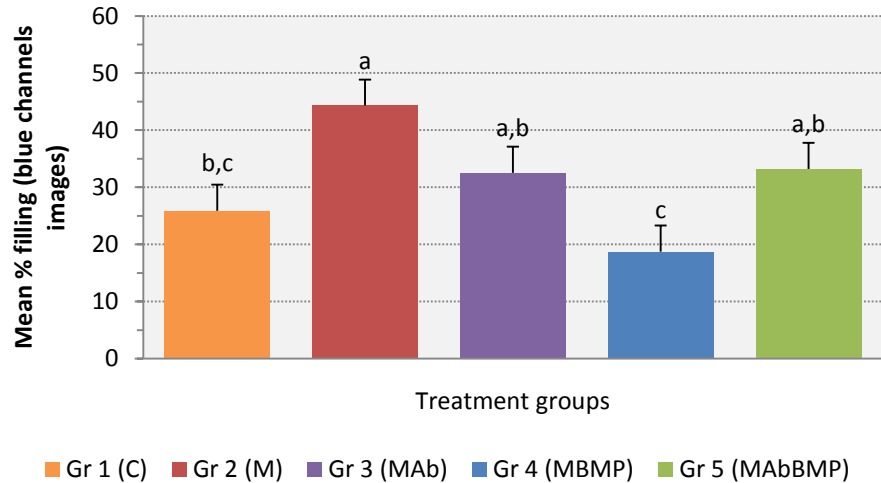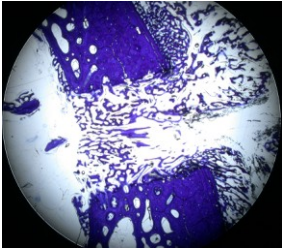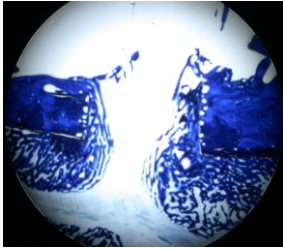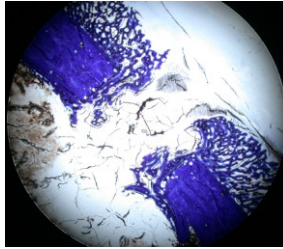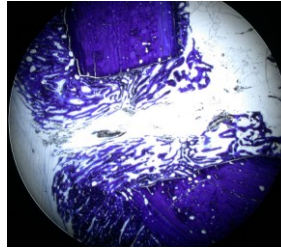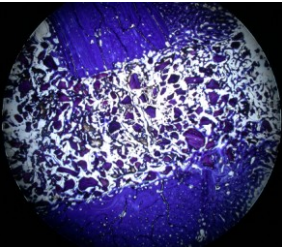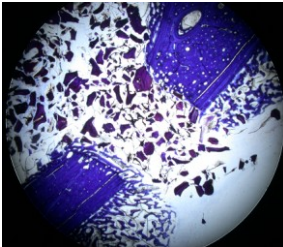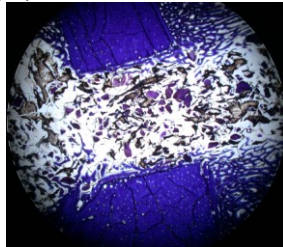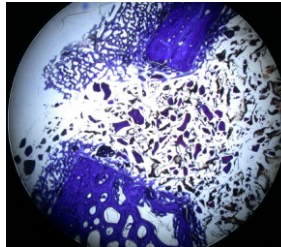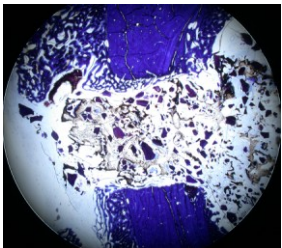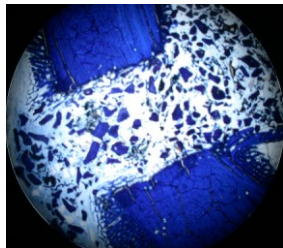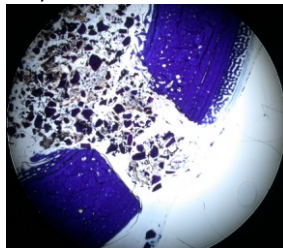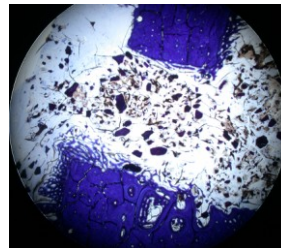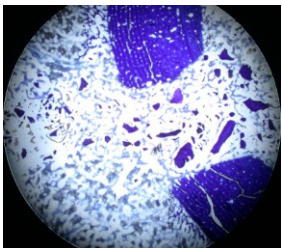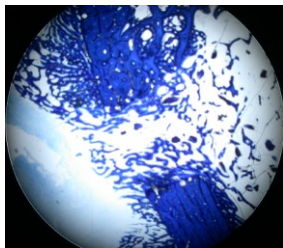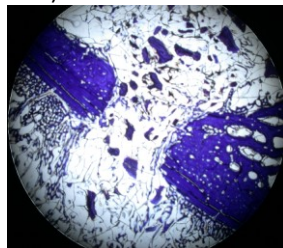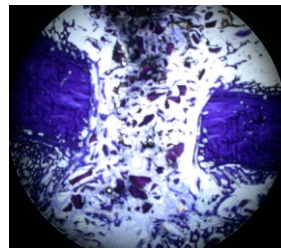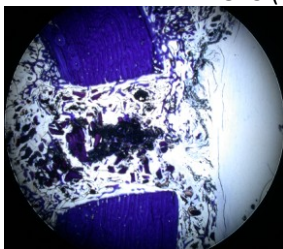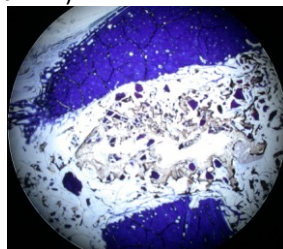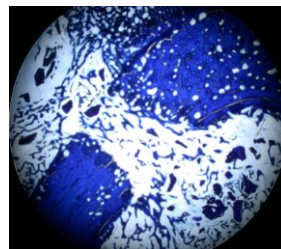
Figure B.18 Mean Percent Filling of Bone Defects Evaluated by Computerized Image Analysis of the Blue Channels Images, Day 30
Bars that share a letter (a-b) are not statistically different at $P < 0.05$.

Table B.1 Photographs of Undecalcified Bone Defects; Toluidine Blue Stained Histological Slides under 2X Objective for All Goats; Day 30

Gr 1 (C)

32 (right)	35 (right)	38 (left)	43 (right)

Gr 2 (M)

42 (right)	44 (left)	47 (right)	48 (left)

Gr 3 (MAb)

39 (left)	40 (left)	41 (left)	45 (right)

Gr 4 (MBMP)

27 (left)	29 (left)	33 (right)	36 (right)

Gr 5 (MAbBMP)

18 (left)	30 (left)	34 (right)	37 (left)

Appendix C - Protocol for Image Analysis Using ImageJ Software

Software: ImageJ 1.42q, Wayne Rasband, National Institutes of Health, USA, http://rsb.info.nih.gov/ij.

Steps:

1. File → open, choose image, click OK.

2. Image → Rotate → Arbitrarily… In the new window, choose the angle of rotation in degrees, check the preview box, then click OK.
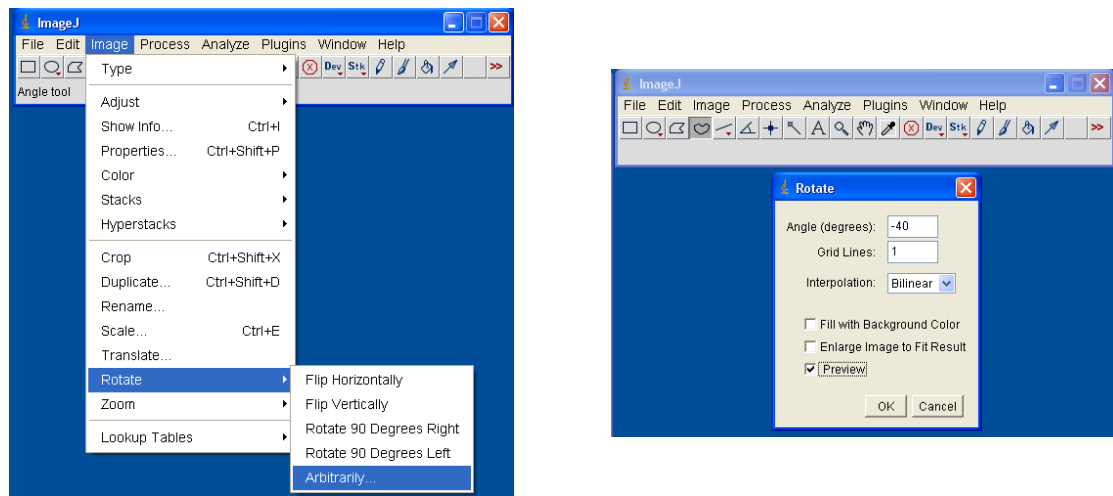
Figure C.1 Image Analysis, Step 2.

3. Using the rectangle selection tool, make a selection of the area to crop. Then, Image → Crop
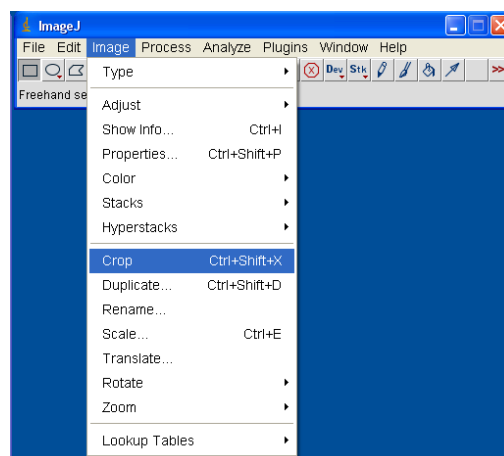
Figure C.2 Image Analysis, Step 3.

4. Process → Substract Background, √check the preview box, then click OK.
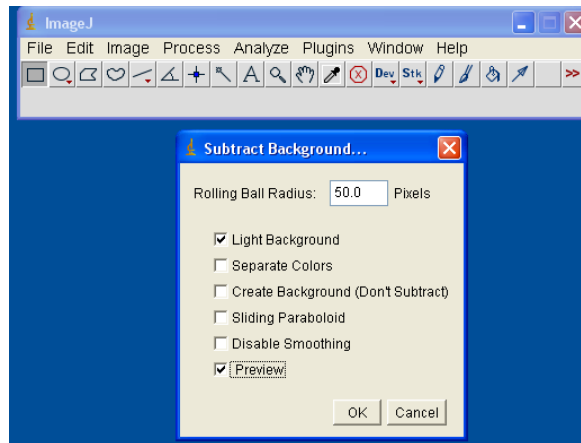
Figure C.3 Image Analysis, Step 4.
The Rolling Ball Radius was kept at 50.0 pixels for each images and the Light Background box was always checked.

5. Image → Adjust → Brightness & Contrast.
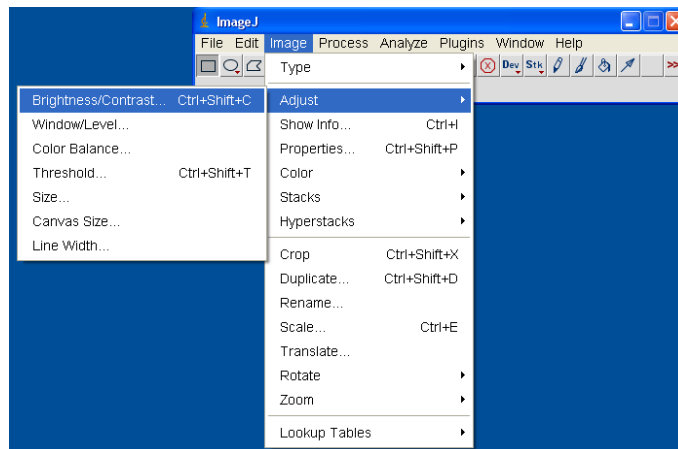
Figure C.4 Image Analysis, Step 5.

6. Click Auto, then click Apply. Close the window.
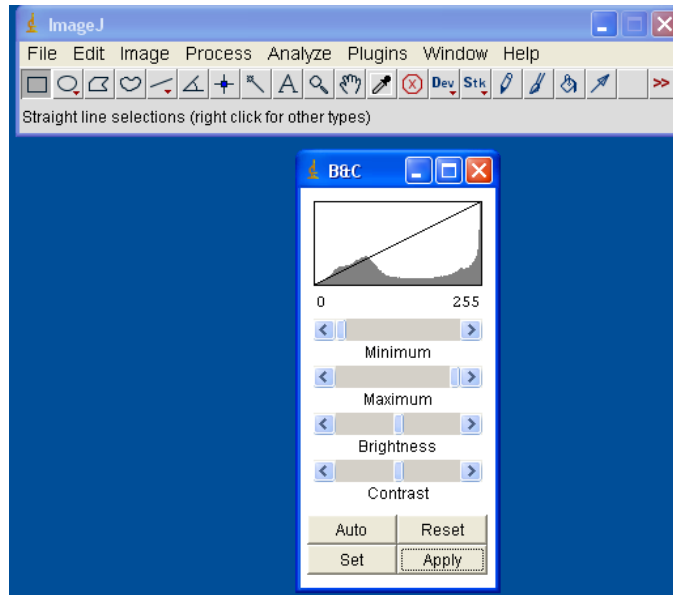
Figure C.5 Image Analysis, Step 6.

7. File → Save As → Tiff… The image was then saved under DSCNxxxx-tagx-1 in file "1. after substract background".
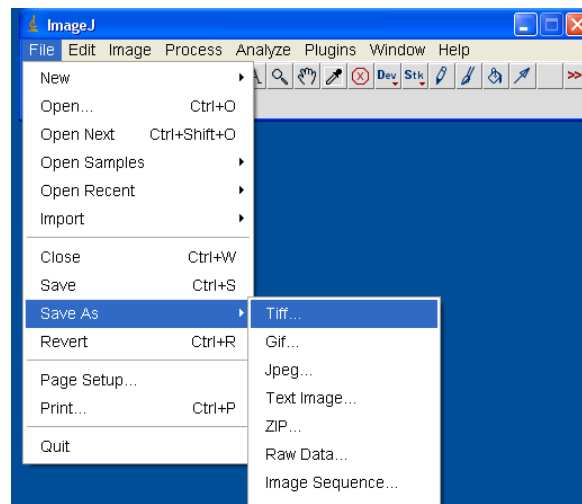
Figure C.6 Image Analysis, Step 7.

8. The width of the bone defect was measured using the line selection tool.
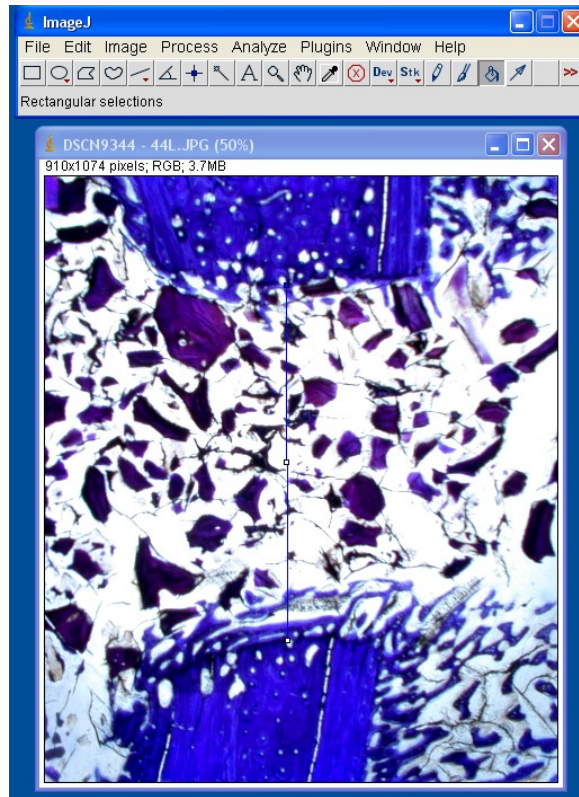
Figure C.7 Image Analysis, Step 8.
Measurement of the bone defect width.

9. Analyse → Set Scale.
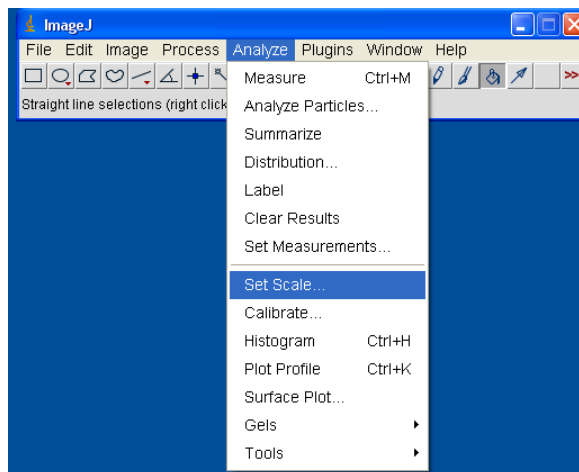
Figure C.8 Image Analysis, Step 9.

10. The length of the line is automatically entered as "Distance in Pixels". Enter the "Known Distance" as 3500 μm (the width of the bone defect). Enter the "Units of Length" as um. Then, click OK.
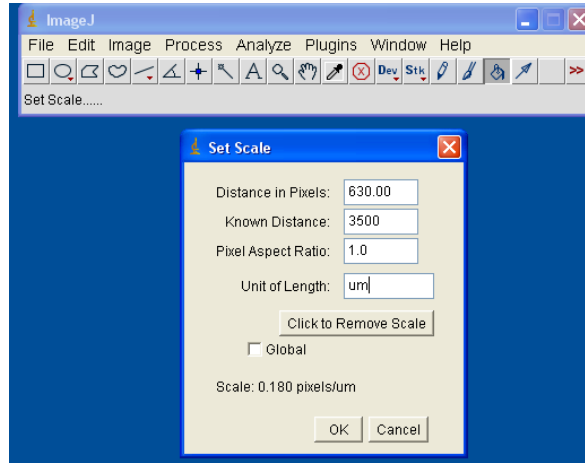
Figure C.9 Image Analysis, Step 10.
The scale was then noted into the data table. (On this example, the scale was 0.180 pixels/μm).

11. Image → Save As → .Tiff The image was then saved under DSCNxxxx-tagx-2 in file "2. after setting scale".

12. Analyse → Tools → Scale Bar…
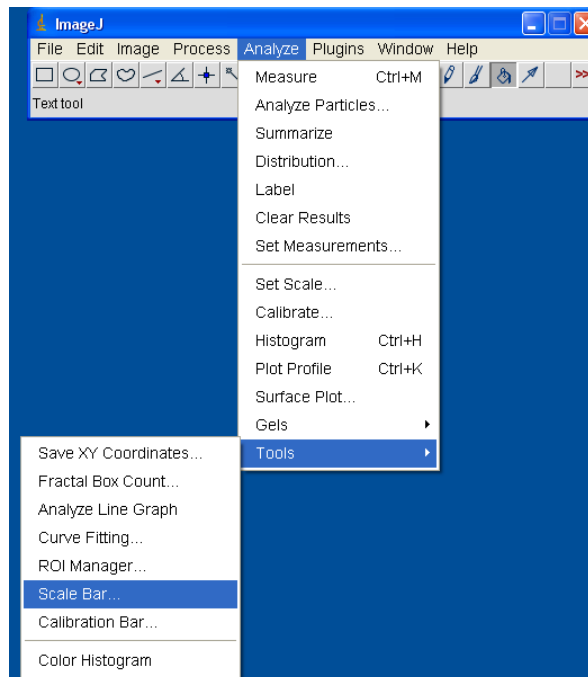
Figure C.10 Image Analysis, Step 12.

13. Replace the parameters as needed. Then, click OK.
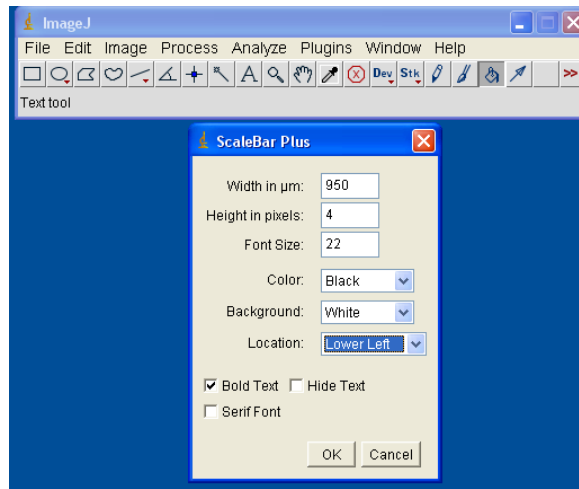
Figure C.11 Image Analysis, Step 13.
For all pictures, the parameters were: Width in μm = 950; Height in pixels = 4; Font size = 22;
Color = Black; Background = White; Location = Lower Left; Bold Text

14. Image → Save As → .Tiff The image was then saved under DSCNxxxx-tagx-3 in file "3. with scale on image".

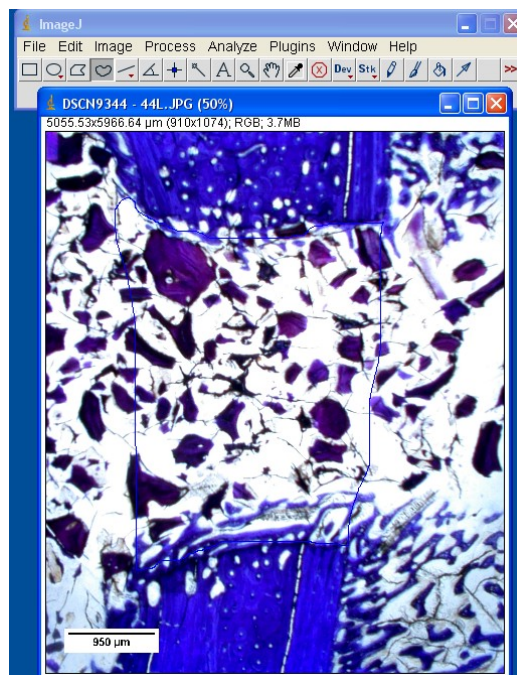15. Select the area of interest (cortical bone defect) using the freehand shape selection tool.

Figure C.12 Image Analysis, Step 15.

16. Image → Type → RGB Stack (to split the image into red, green and blue channels)
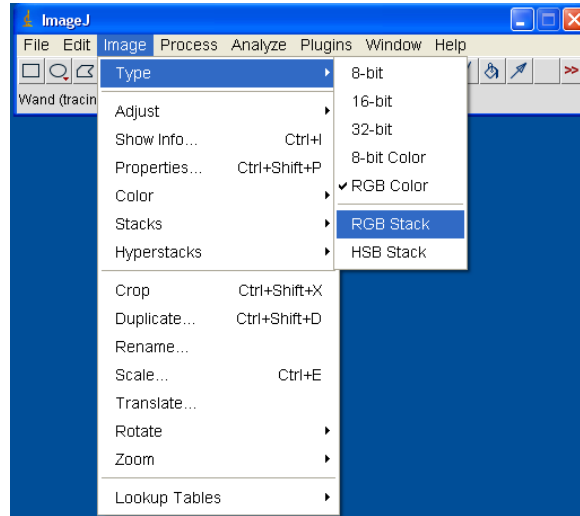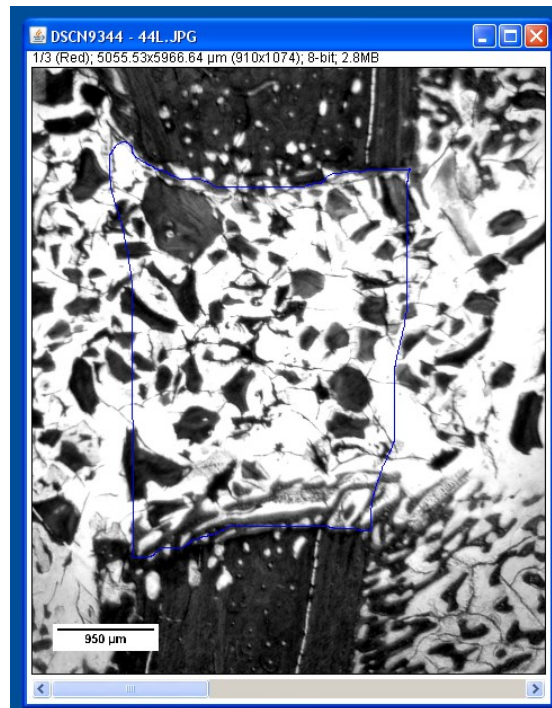

Figure C.13 Image Analysis, Step 16.

Figure C.14 Image Splitted into Red Channels.
An area of interest is highlighted using the selection tool.

17. Image → Save As → .Tiff The image was then saved under DSCNxxxx-tagx-4 in file "4. stacks RGB images".
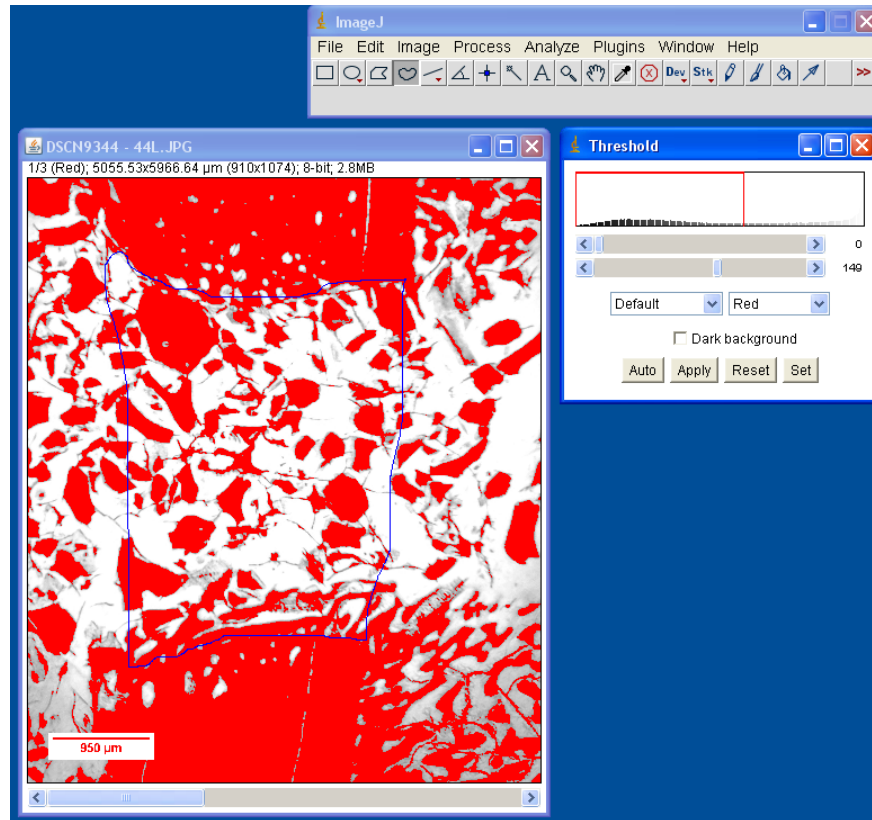
18. Image → Adjust → Threshold

Figure C.15 Image Analysis, Step 18.
The threshold was always adjusted to 149 for each red channel images.

19. Analyse → Set Measurements. √ Check "Area", "Area Fraction", "Limit to Threshold" and "Display Label". Then, click OK.
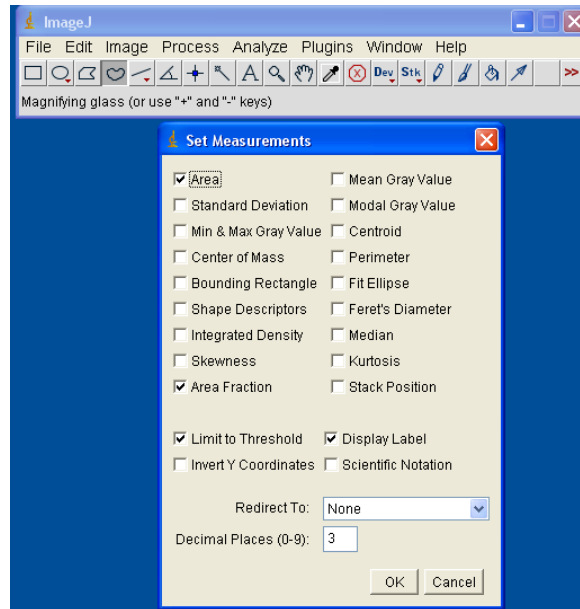
Figure C.16 Image Analysis, Step 19.

20. Press "m" (or Analyse → Measure) to display area and % area in the Results window.

21. Select the green channel by moving the lower bar on the picture and repeat steps 18 to 20. The threshold was always adjusted to 149 for each green channel images.

22. Select the blue channel by moving the lower bar on the picture and repeat steps 18 to 20. The threshold was always adjusted to 200 for each blue channel images.

23. Right click in the result window and "Save As" .doc or "Copy" to another text file.